86-2

A BANDWIDTH EFFICIENT FREQUENCY-HOPPED SPREAD SPECTRUM MODULATION STUDY

FINAL REPORT

PREPARED FOR THE DEPARTMENT OF COMMUNICATIONS

D.S.S. CONTRACT
OST85-00190

BY

P.H. WITTKE
P.J. McLANE
Y.M. LAM
S.J. SIMMONS

MARCH 1986

Queen's University at Kingston
Department of Electrical Engineering

CRC-DP-CR-86-002

A BANDWIDTH EFFICIENT FREQUENCY-HOPPED SPREAD SPECTRUM MODULATION STUDY

by

P.H. Wittke

P.J. McLane

Y.M. Lam

S.J. Simmons

Report No. 86-2

Final Report

Prepared for

The Department of Communications

Under DSS Contract No. OST85-00190

DSS no. 24ST 36001-5-3547

Department of Electrical Engineering

Queen's University

Kingston, Ontario, Canada

March, 1986

TABLE OF CONTENTS

SUMMARY

A study has been carried out of frequency-hopped spread spectrum systems in which the modulation between hops is a phase-continuous coherent band efficient modulation. The bandwidth occupied by the dehopped, modulated signal is of prime importance as it relates directly to the processing gain, the number of possible users and the degree of anti-jam protection achievable. Thus there appears a possible advantage in the use of a bandwidth efficient coherent frequency modulation scheme for the transmission of a number of bits during each hop interval. In this contract period, the band occupancy and spectral study has been completed with an examination of the case where the hopping frame is synchronous with the baud timing. Examples have been calculated for a range of band-efficient modulations including MSK, duobinary and Tamed FM. Results on the power density spectra of frequency-hopped signals with various partial response encodings and pulse shaping, and different hop lengths show that in general the spectrum becomes more compact with lower sidelobes and approaches that of the CPM signal without hopping, as the length of the hop interval increases. It is found that the use of higher order partial response polynomials and pulse shaping, become effective in bandwidth and sidelobe reduction as the hop interval increases.

Three algorithm based noncoherent receivers have been derived. A maximum likelihood receiver that is optimum over a single hop interval has been studied in greatest detail. It has the simplest receiver structure and decoding algorithm, and it can be used for

sequence estimation on a hop-by-hop basis. As well, the error performance of this receiver has been analysed. It has higher error probability at the beginning and at the end of a hop. However, if some channel throughput can be sacrificed, known symbols can be transmitted at the beginning and end of a hop to force a merge in the modulation trellis, and to improve error performance.

The MLSE receiver that detects a general frequency-hopped signal has been obtained. It has the same structure as the one that detects on a hop-by-hop basis but it has a more complicated decoding algorithm. However, simplification of the decoding algorithm is possible when the length of the hop interval is much greater than the length of the frequency pulse. The receiver operates generally in the same manner as the single hop receiver, but it has a subprocedure for metric calculation across each frequency hop and relies on the assumption that a merge in the trellis will occur well before the end of a hop.

An additional simplified suboptimum receiver has been found. For this receiver a different structure is required with a simpler decoding algorithm and reduced memory and computation requirements.

The other main area of research under the contract has been in the development and application of trellis coding to hopped spread spectrum systems. The common applications of coding and coded modulations have been to the additive Gaussian noise channel where a coherent modulation and demodulation has been possible. For example the Trellis Codes of Ungerboeck, have been applied to 8-phase PSK and 16 point Quadrature Amplitude Modulation, to achieve coding gains of the order of 3 dB with no penalty in transmission rate. However, for

hopped communications in the EHF band, coherent techniques do not appear possible and it is a challenge to find effective coding and decoding techniques that use noncoherent detection. In this report, the principles and first results are presented on a coded Noncoherent Frequency Shift Keying (NC-FSK) modulation that promises coding gains of the order of 3-4 dB as has been achieved with trellis codes and coherent systems. In addition, because the basic modulation is a noncoherent M-ary FSK, the use of existing spectrum analyzer receivers appears possible.

I. HOPPED SPREAD SPECTRUM SYSTEMS WITH BAND-EFFICIENT MODULATIONS

1.INTRODUCTION

In recent years, there has been an increase in Electronic Counter-Counter-Measures (ECCM) in military satellite communications (MILSATCOM). The trend in MILSATCOM has been to communications in the Extremely High Frequency (EHF) Band using frequency-hopping techniques.

Frequency-hopping techniques typically achieve much wider spread spectrum bandwidth than direct sequence modulation techniques, resulting in higher processing gain, which is defined as the ratio of the hopped bandwidth to the information bandwidth [1]. Frequency bands which are unusually noisy, are jammed, or exhibit severe fading can be hopped around. Frequency-hopping is hence the preferred spread spectrum technique over direct sequence tehcniques when the information signal is to be spread over the wide bandwidths available at the EHF band.

Consider a frequency-hopped spread spectrum system that is required to handle high speed data. Thus although on an absolute scale the frequency-hopping may be fast, relative to the data rate we can have a slow hopping situation, that is, many or at least several bits of data are transmitted per chip interval. Slow frequency hopping allows many data bits to be transmitted per hop and the resulting transmitter and receiver are simpler and less expensive than for faster frequency-hopping. Due to the wideband nature of the data and the desire to enhance the spread spectrum processing gain as much as possible, the modulated bandwidth of the data signal is of considerable concern. A requirement exists to make use of a bandwidth ef-

ficient modulation scheme in order to both enhance the ECCM performance and allow multiple users.

The bandwidth occupied by the dehopped, modulated signal is of prime importance and relates directly to the degree of anti-jam protection achievable. Thus there appears a possible advantage in the use of a bandwidth efficient coherent frequency modulation scheme for the transmission of a number of bits during each hop interval. It has been shown that continuous phase modulation (CPM) schemes are band efficient and also power efficient when detected coherently [2]. Correlative encoding [3], also termed partial response signaling [4], can be used for spectral shaping and to gain spectral efficiency. Furthermore, baseband pulse shaping can be used to obtain more compact spectra as well. A transmitter for this slow frequency-hopping correlative encoded digital FM spread spectrum system is shown in Fig. 1.

2.SPECTRAL ANALYSIS

2.1 INTRODUCTION

Since the bandwidth occupied by the dehopped, modulated signal is of prime importance and relates directly to the degree of protection against jamming achievable, it is thus important to examine the power density spectrum of the modulated signal. The signal is basically a hopped signal with a random hop occurring after every N transmitted symbols or every NT seconds. During any one hop interval, the modulation is assumed to be coherent frequency modulation, with correlative or partial response encoding and shaping of the modulating

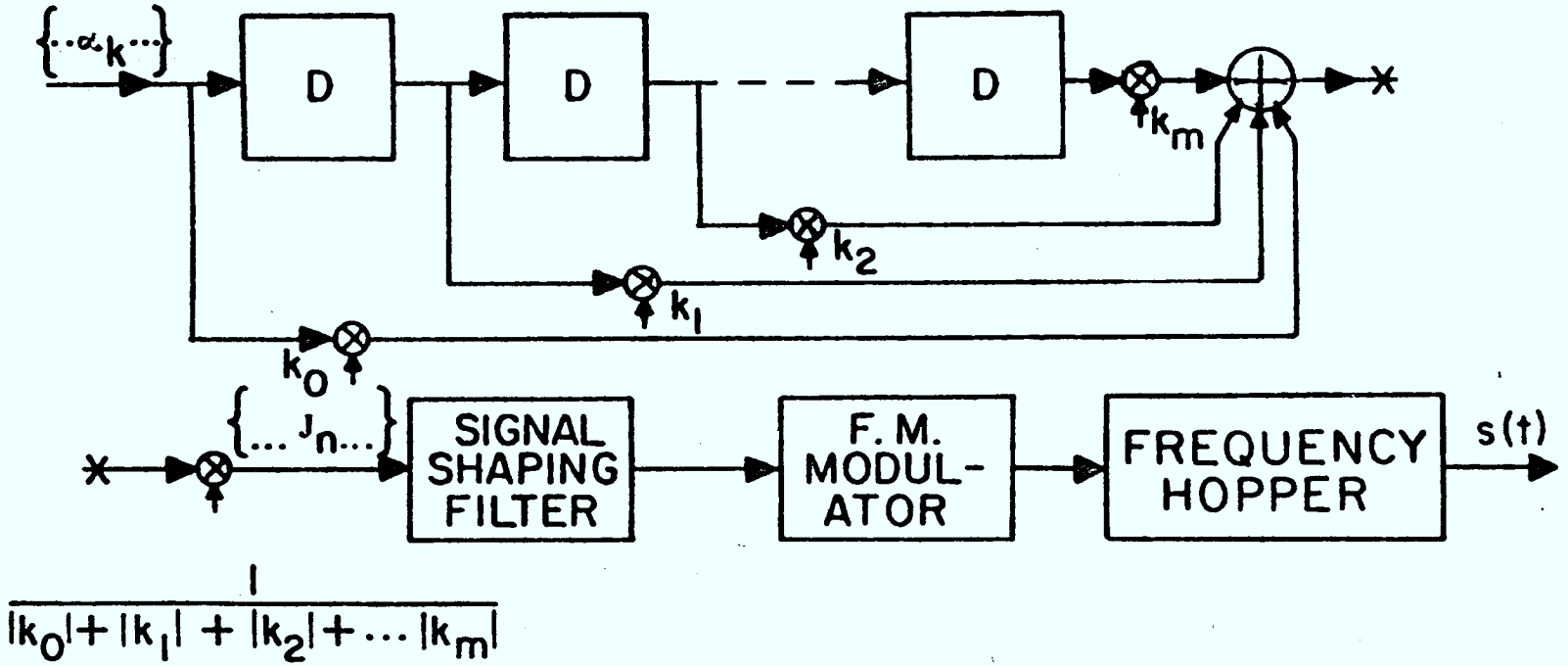

Fig. 1. Bandwidth Efficient Frequency-hopped Transmitter.

pulses permissible. The frequency-hopped correlative encoded CPM signal can be represented by

$$s(t) = \sum_{i=-\infty}^{\infty} p(t-iNT) \cos[2\pi f_i t + \psi(t,\underline{\alpha}) + \theta_i] \qquad (2.1)$$

where N is the number of symbols in a hop interval,

T is the symbol interval,

$$p(t) = \begin{cases} 1 & 0<t<NT \\ 0 & \text{elsewhere} \end{cases}$$

f_i is the carrier frequency of the i^{th} hop,

θ_i is the random initial phase at the beginning of the i^{th} hop, and the θ_i's are assumed to be independent random variables uniformly distributed from 0 to 2π,

$\psi(t,\underline{\alpha})$ is the information carrying phase function given by

$$\psi(t,\underline{\alpha}) = 2\pi h \sum_{n=-\infty}^{\infty} \alpha_n q(t-nT) \qquad (2.2)$$

where h is the modulation index,

$$\underline{\alpha} = \{ \ldots\ldots \alpha_{-2}\ \alpha_{-1}\ \alpha_0\ \alpha_1\ \alpha_2\ \ldots\ldots \}$$

is the sequence of uncorrelated input data symbols. For an M-ary scheme, each data symbol can take any of the values $\alpha_i = \pm 1, \pm 3, \ldots\ldots, \pm(M-1)$ with equal probability. q(t) is the phase response given by

$$q(t) = \int_{-\infty}^{t} g(\tau)\, d\tau \qquad (2.3)$$

For a correlative encoder with a partial response system (PRS)

polynomial given by

$$F(D) = (1/C)\ (k_0 + k_1 D + k_2 D^2 + \ldots + k_m D^m) \tag{2.4}$$

where $$C = \sum_{\ell=0}^{m} |k_\ell| \tag{2.5}$$

the frequency pulse g(t) is given by

$$g(t) = (1/C) \sum_{i=0}^{m} k_i\ b(t-iT) \tag{2.6}$$

b(t) is the baseband pulse with a duration of one symbol interval. Spectral shaping can be accomplished by the choice of system polynomial F(D) and by using various baseband pulse shapes such as the raised cosine.

The length of the frequency pulse g(t) is then L=m+1 symbol intervals. q(t) is normalized such that

$$q(LT) = 1/2 \tag{2.7}$$

2.2 SPECTRAL ANALYSIS

There are various methods of calculating the power density spectrum for digital FM [5]. Among these methods, the autocorrelation method [6], is straightforward and easy to to use.

The complex baseband equivalent signal for the dehopped signal is simply

$$u(t) = \sum_{i=-\infty}^{\infty} \exp\{j\theta_i\} p(t-iNT)\ e^{j\psi(t,\underline{a})} \tag{2.8}$$

The complex baseband autocorrelation function is given by

$$R_u(t,t+\tau) = E\{ u^*(t)\, u(t+\tau)\}$$

$$= E\{ \sum_{i=-\infty}^{\infty} \exp\{-j\theta_i\} p(t-iNT)\, e^{-j\psi(t,\underline{\alpha})} \cdot$$

$$\cdot \sum_{\ell=-\infty}^{\infty} \exp\{j\theta_\ell\} p(t+\tau-\ell NT)\, e^{j\psi(t+\tau,\underline{\alpha})} \}$$

$$= E\{ \sum_{i=-\infty}^{\infty} \sum_{\ell=-\infty}^{\infty} \exp\{j(\theta_\ell-\theta_i)\}\, p(t-iNT)\, p(t+\tau-\ell NT) \cdot$$

$$\cdot e^{j[\psi(t+\tau,\underline{\alpha})-\psi(t,\underline{\alpha})]} \} \qquad (2.9)$$

Since the θ_i's are uniformly distributed on $[0,2\pi]$ and are statistically independent

$$E\{\exp[j(\theta_\ell-\theta_i)]\} = \delta_{i,\ell} \qquad (2.10)$$

Hence,

$$R_u(t,t+\tau) = \sum_{i=-\infty}^{\infty} p(t-iNT)\, p(t+\tau-iNT)\, R_{CPM}(t,t+\tau) \qquad (2.11)$$

where $R_{CPM}(t,t+\tau)$ is the complex baseband autocorrelation function of the pure CPM signal without any frequency-hopping and is given by

$$R_{CPM}(t,t+\tau) = E\{e^{j[\psi(t+\tau,\underline{\alpha})-\psi(t,\underline{\alpha})]}\}$$

$$= E\{e^{j2\pi h \sum_{n=-\infty}^{\infty} \alpha_n [q(t+\tau-nT)-q(t-nT)]}\} \qquad (2.12)$$

The sum in the exponent in (2.12) can be written as a product and averaged with respect to the sequence $\underline{\alpha}$, assuming that the M-ary data are independent and are transmitted with equal probability 1/M. Then

$$R_{CPM}(t,t+\tau) = \prod_{n=-\infty}^{\infty} \{(2/M) \sum_{j=1}^{M/2} \cos 2\pi h(2j-1)[q(t+\tau-nT)-q(t-nT)]\} \qquad (2.13)$$

Since the frequency pulse g(t) is of finite duration LT, if we let $\tau = aT+\tau'$, where a is a positive integer and $0 \leq \tau' \leq T$, the infinite product in (2.13) simplifies to

$$R_{CPM}(t,t+\tau) = R_{CPM}(t,t+aT+\tau')$$

$$= \prod_{n=1-L}^{a+1} \{(2/M) \sum_{j=1}^{M/2} \cos 2\pi h(2j-1)[q(t+\tau'-(n-a)T)-q(t-nT)]\} \tag{2.14}$$

Although the time average of $R_{CPM}(t,t+\tau)$ can be taken over a symbol interval T, the time average of $R_u(t,t+\tau)$ has to be taken over NT in order to eliminate the dependence of $R_u(t,t+\tau)$ on the t variable.

$$R_u(\tau) = \frac{1}{NT} \int_0^{NT} R_u(t,t+\tau)\, dt$$

$$= \frac{1}{NT} \int_0^{NT} \sum_{i=-\infty}^{\infty} p(t-iNT)\, p(t+\tau-iNT)\, R_{CPM}(t,t+\tau)\, dt$$

$$= \frac{1}{NT} \int_{-\infty}^{\infty} p(t)p(t+\tau)\, R_{CPM}(t,t+\tau)\, dt$$

$$= \begin{cases} \frac{1}{NT} \int_0^{NT-\tau} R_{CPM}(t,t+\tau)\, dt & NT > \tau > 0 \\ \frac{1}{NT} \int_{-\tau}^{NT} R_{CPM}(t,t+\tau)\, dt & -NT < \tau < 0 \\ 0 & |\tau| > NT \end{cases} \tag{2.15}$$

Since $R_{CPM}(t,t+\tau)$ as given by Eq.(2.14) is periodic in t with period T, if $0 \leq \tau \leq NT$ and we let $\tau = aT + \tau'$, where a is a positive integer and $0 < \tau' < T$,

$$R_u(\tau) = R_u(aT+\tau')$$

$$= \frac{1}{NT} \int_0^{(N-a)T-\tau'} R_{CPM}(t,t+aT+\tau')\, dt$$

$$= \frac{1}{NT} \left\{ \int_0^{(N-a-1)T} R_{CPM}(t,t+aT+\tau')dt + \int_{(N-a-1)T}^{(N-a)T-\tau'} R_{CPM}(t,t+aT+t')dt \right\}$$

$$= \frac{1}{NT} \left\{ \sum_{k=0}^{N-a-2} \int_{kT}^{(k+1)T} R_{CPM}(t,t+aT+\tau')dt \right.$$

$$\left. + \int_{(N-a-1)T}^{(N-a)T-\tau'} R_{CPM}(t,t+aT+\tau')dt \right\}$$

$$= \frac{1}{NT} \left\{ (N-a-1)T \; R_{CPM}(aT+\tau') + \int_0^{T-\tau'} R_{CPM}(t,t+aT+\tau')d \right\}$$

$$= \frac{N-a-1}{N} R_{CPM}(aT+\tau') + \frac{1}{NT} \int_0^{T-\tau'} R_{CPM}(t,t+aT+\tau')dt \qquad (2.16)$$

Since the CPM autocorrelation function as given by (2.14) is real and therefore an even function of τ, we have

$$R_u(-\tau) = R_u(\tau) \qquad (2.17)$$

Hence, we have

$$R_u(\tau) = R_u(aT+\tau')$$

$$= \frac{N-a-1}{N} R_{CPM}(aT+\tau') + \frac{1}{NT} \int_0^{T-\tau'} R_{CPM}(t,t+aT+\tau')dt \qquad (2.18)$$

$$aT + \tau' = |\tau|,$$

where $0 < \tau' < T$,

and $a=0,1,2, \ldots,N-1$

$$R_u(\tau) = 0 \qquad |\tau| > NT$$

where $R_{CPM}(aT+\tau')$, which is the autocorrelation of the CPM signal without frequency-hopping, is given by

$$R_{CPM}(aT+\tau') = \frac{1}{T} \int_0^T R_{CPM}(t,t+aT+\tau')dt \qquad (2.19)$$

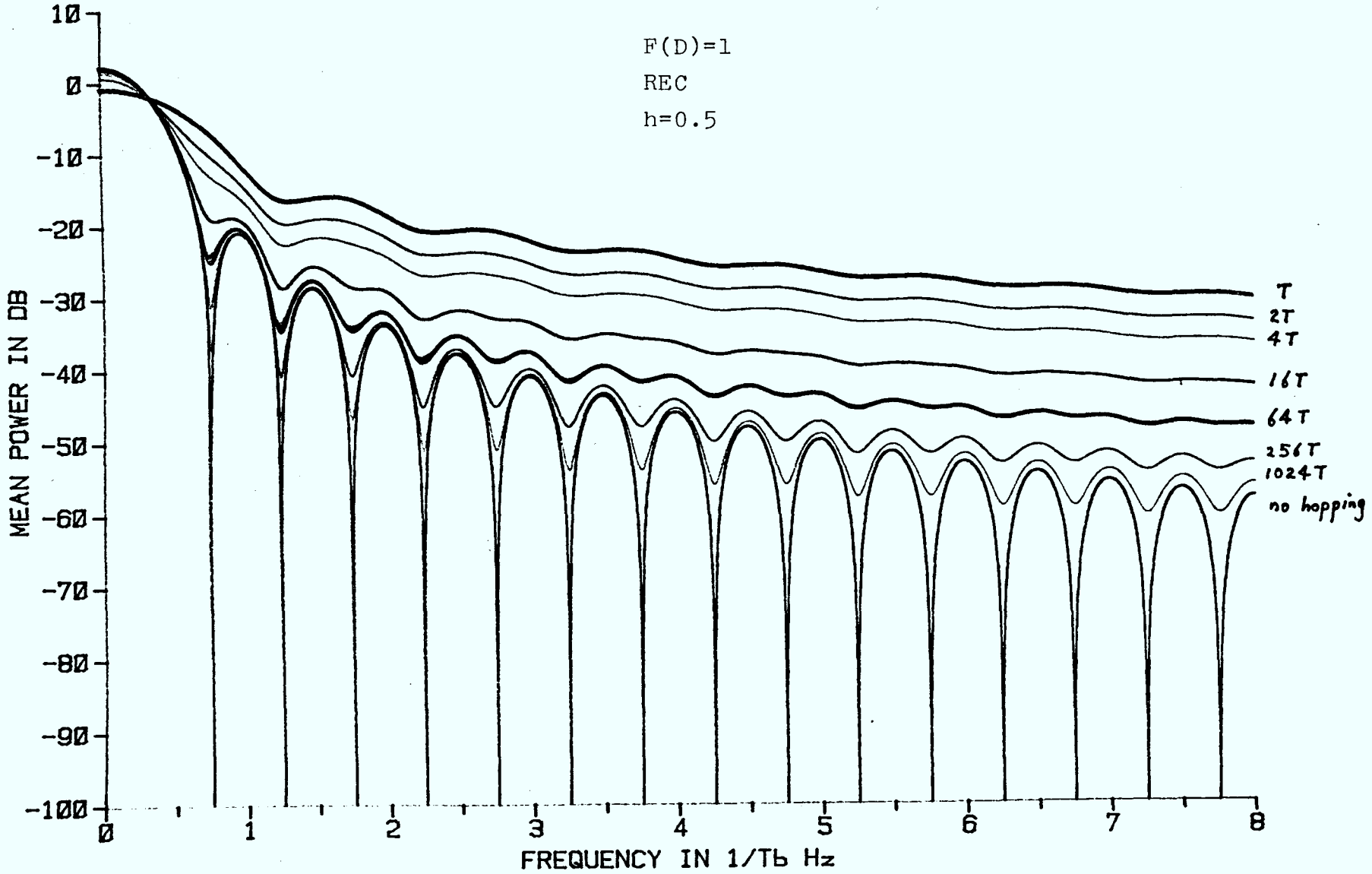

Fig.2 Hopped MSK

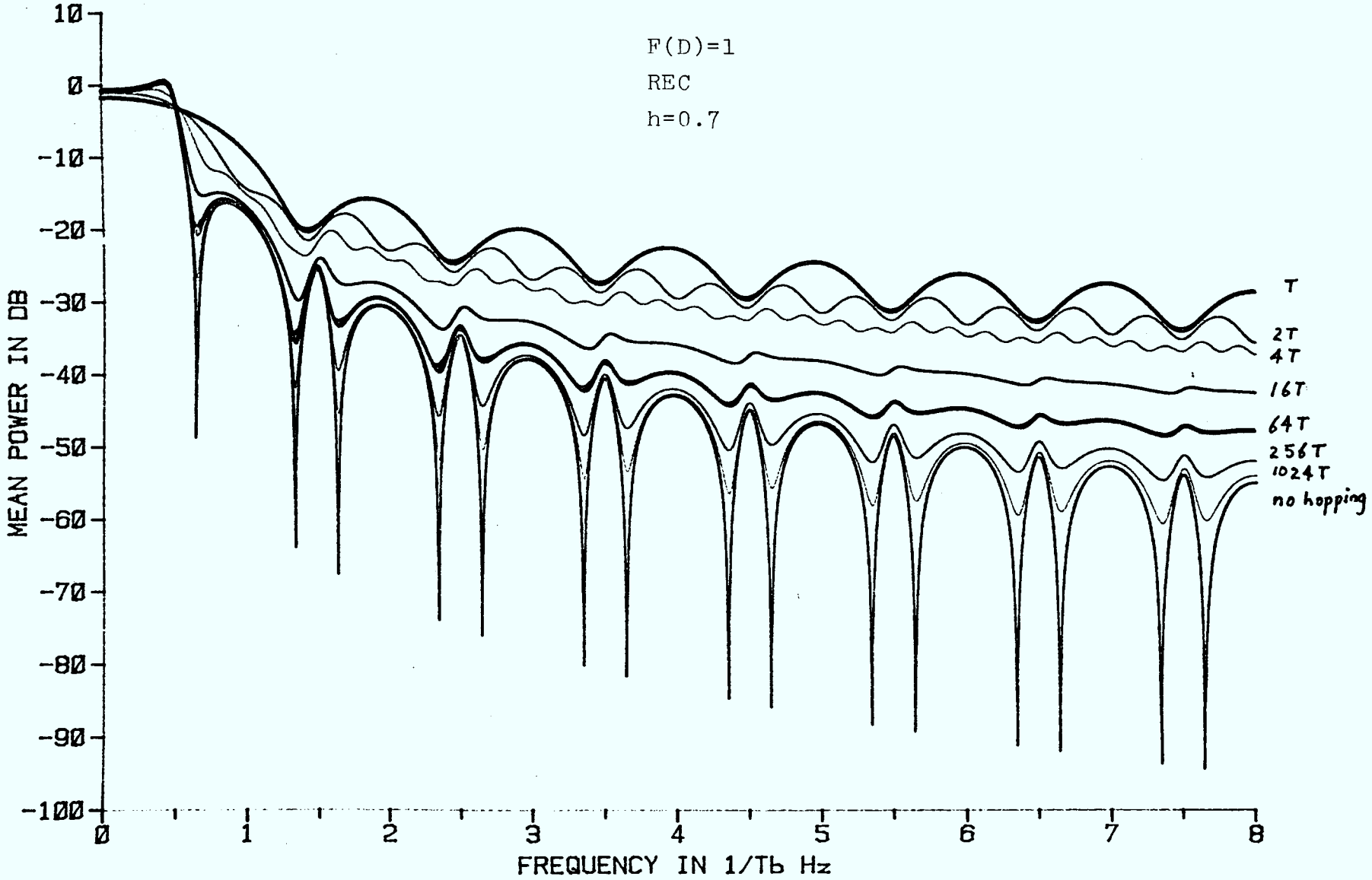

Fig.3 Hopped CPFSK, h=0.7

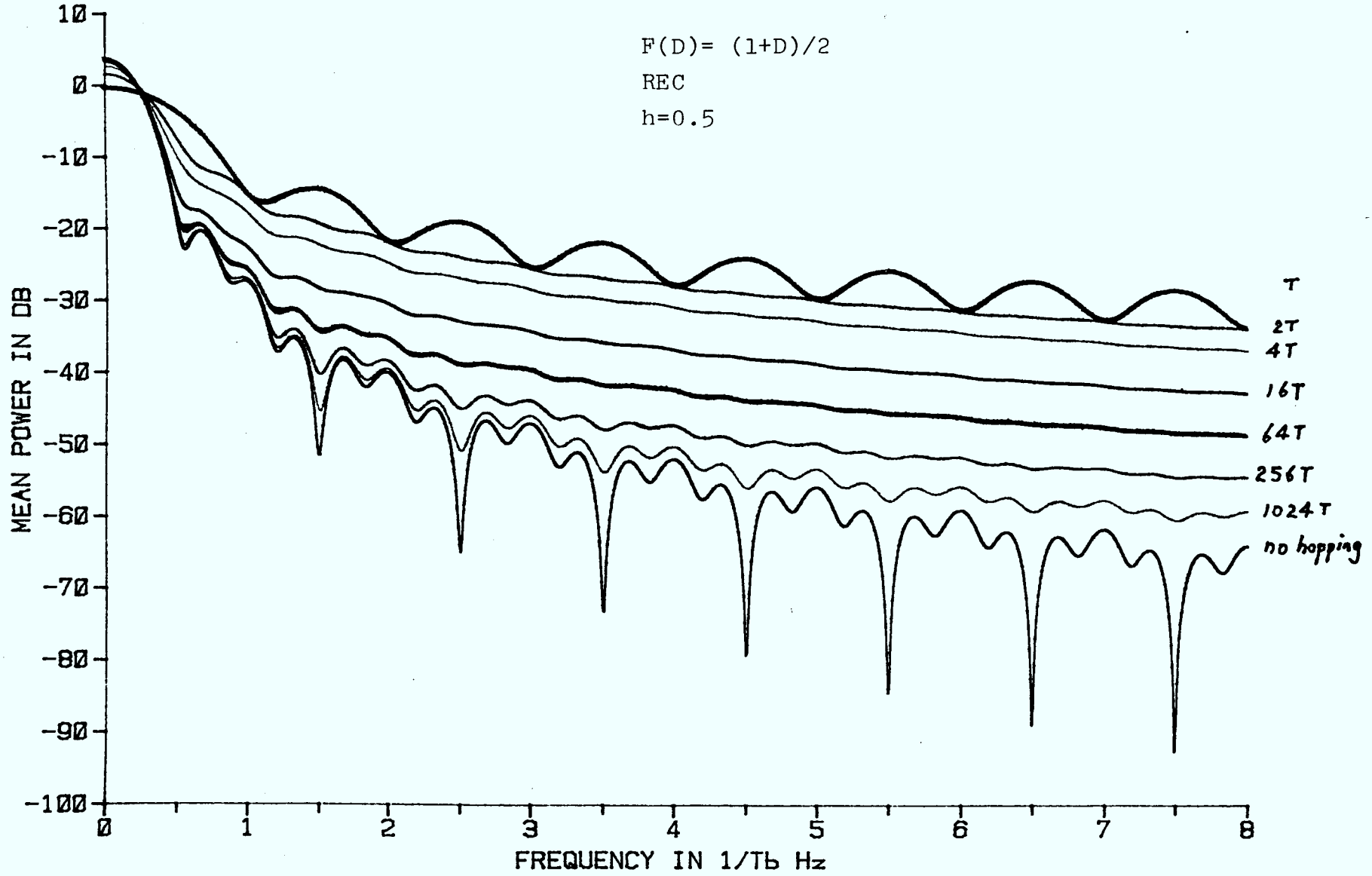

Fig.4 Hopped Duobinary MSK

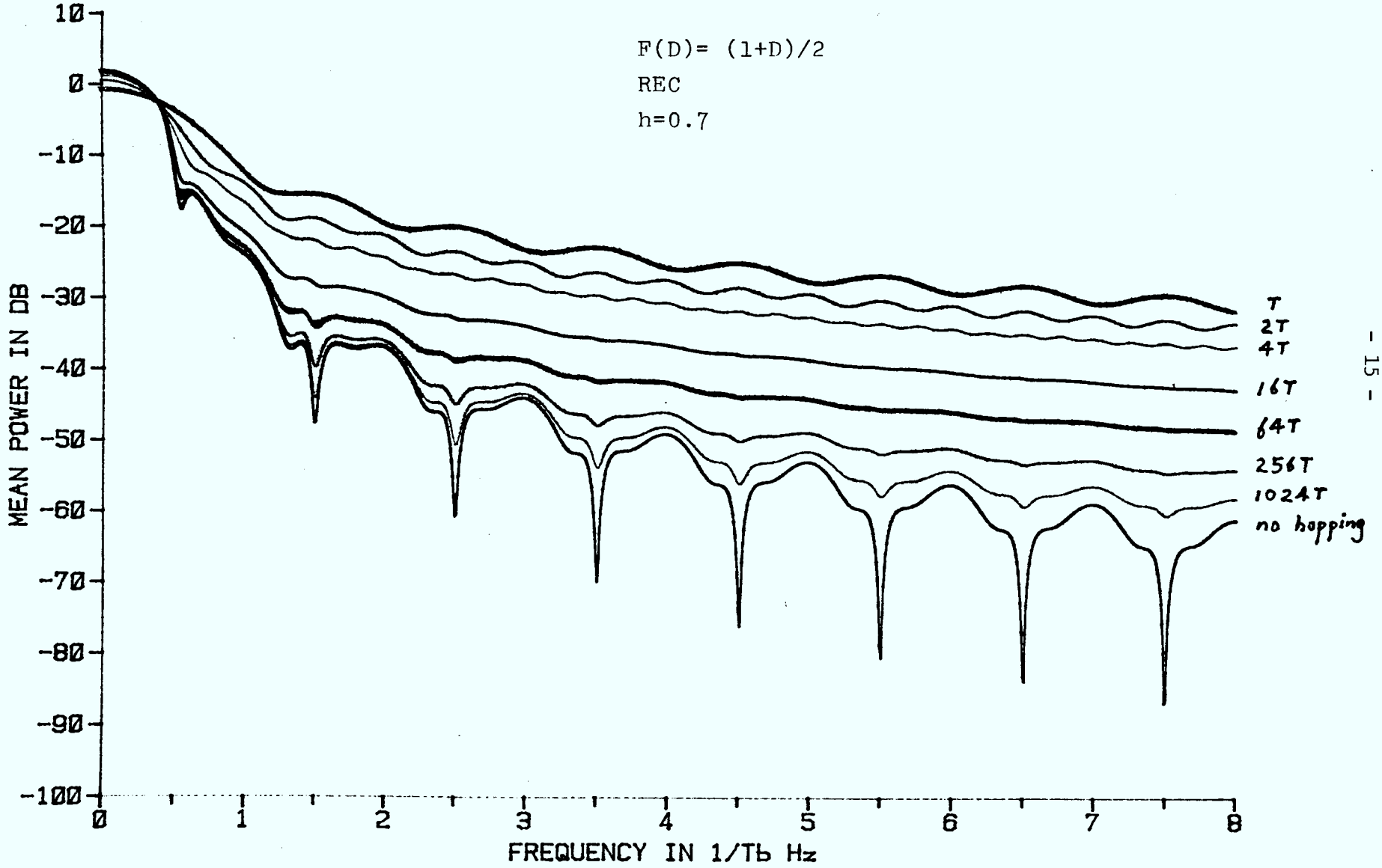

Fig.5 Hopped Duobinary FSK, h=0.7

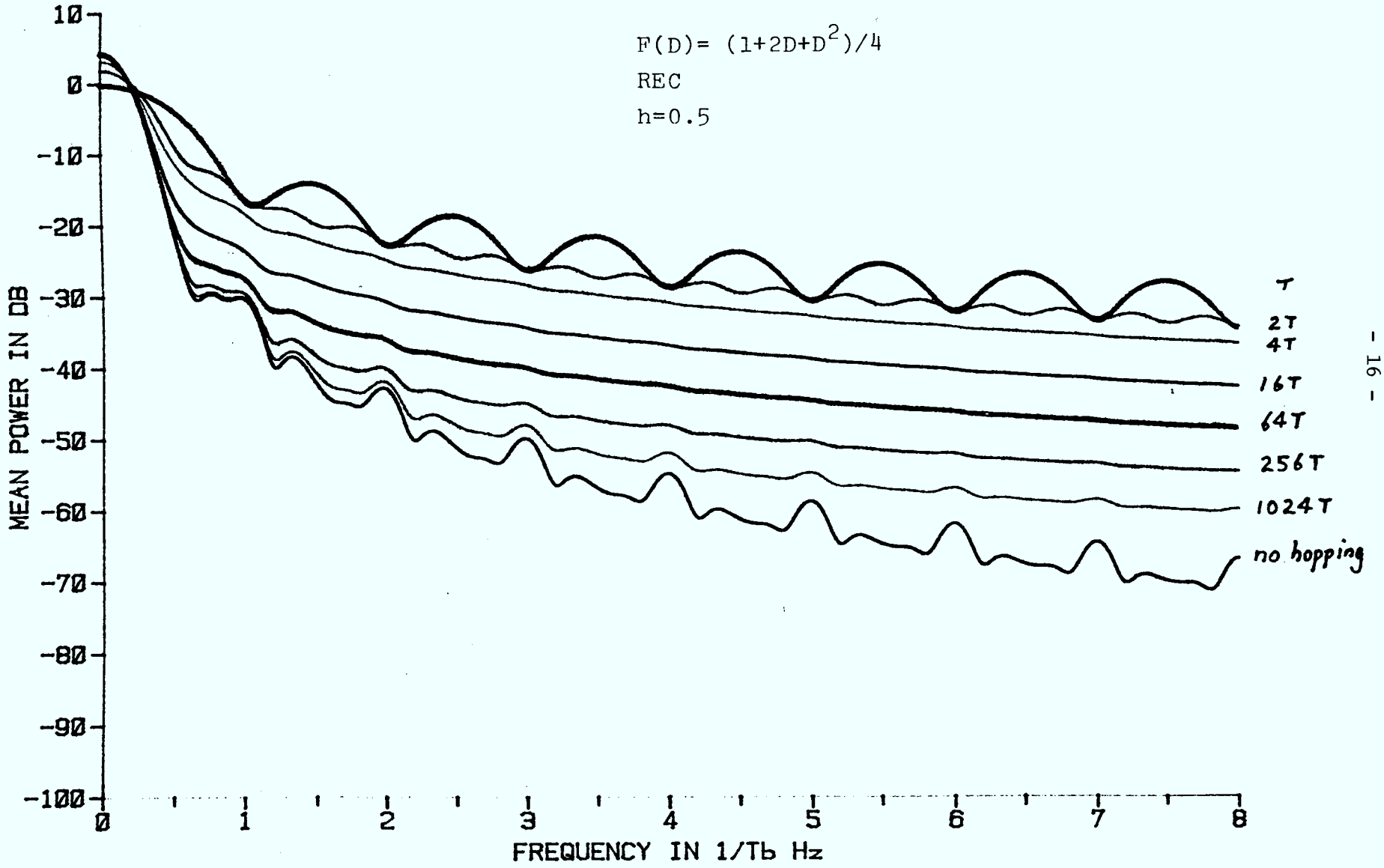

Fig.6 Hopped Tamed FM, h=0.5

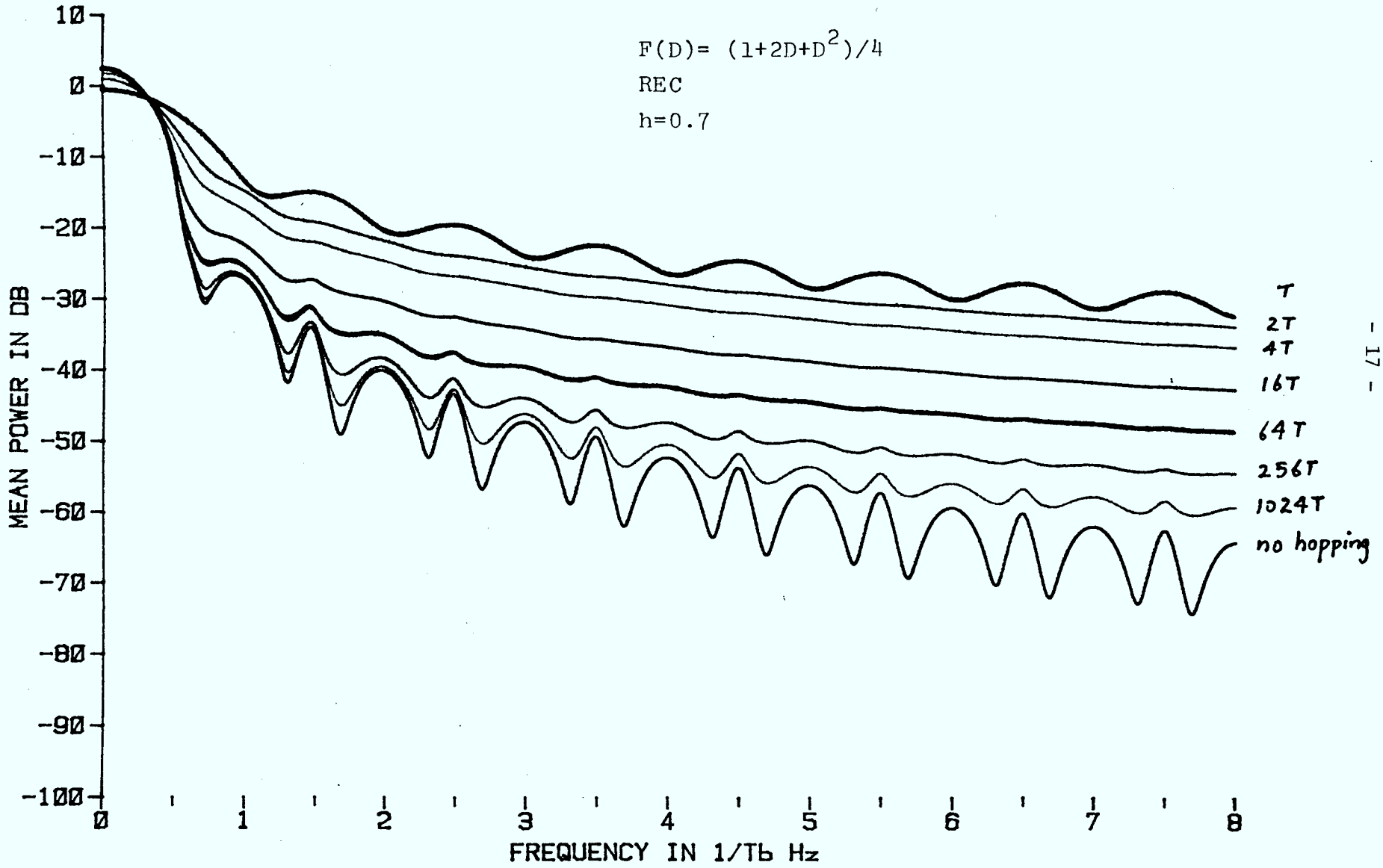

Fig.7 Hopped Tamed FM, h=0.7

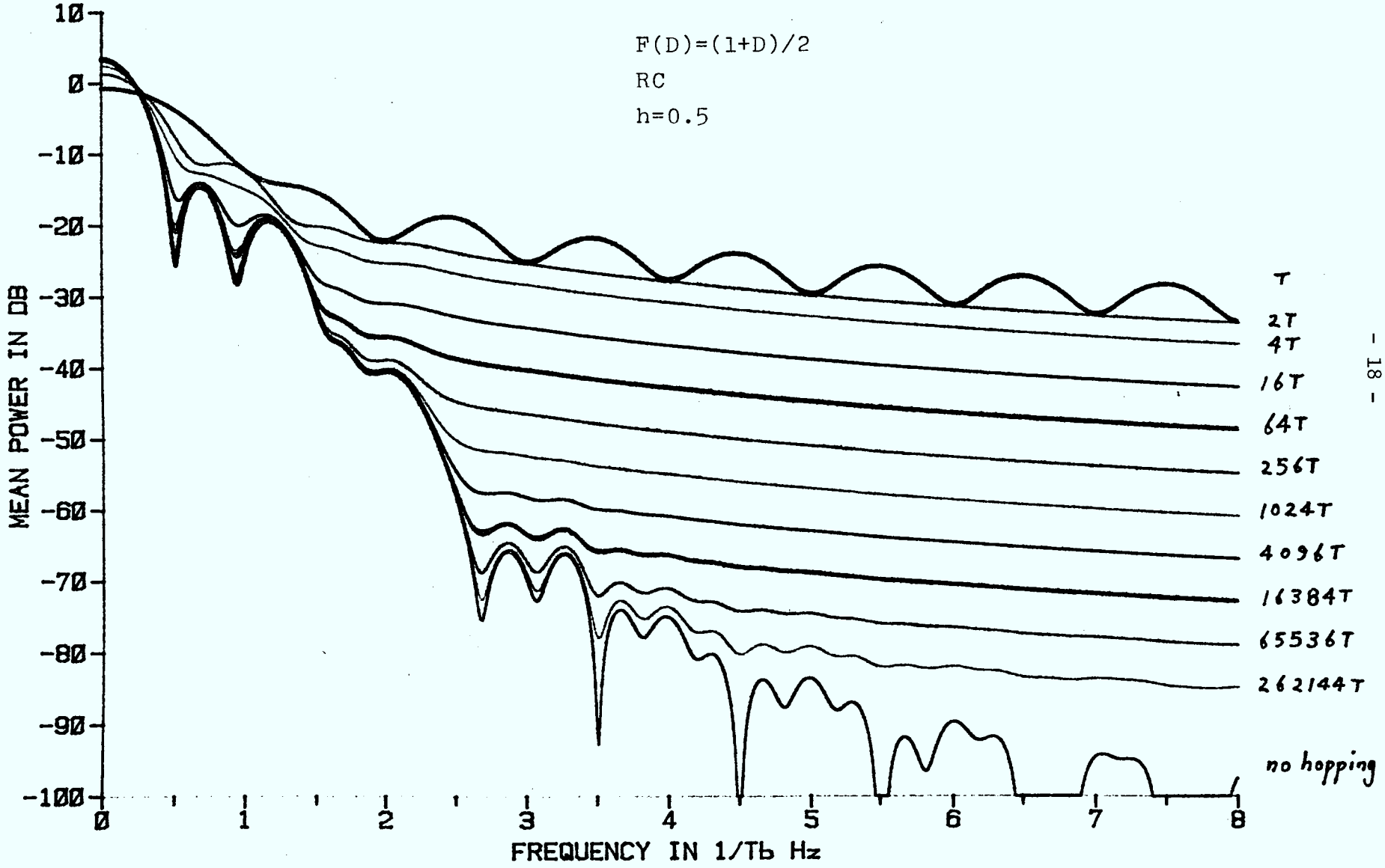

Fig.8 Hopped Duobinary MSK with raised cosine pulse shaping

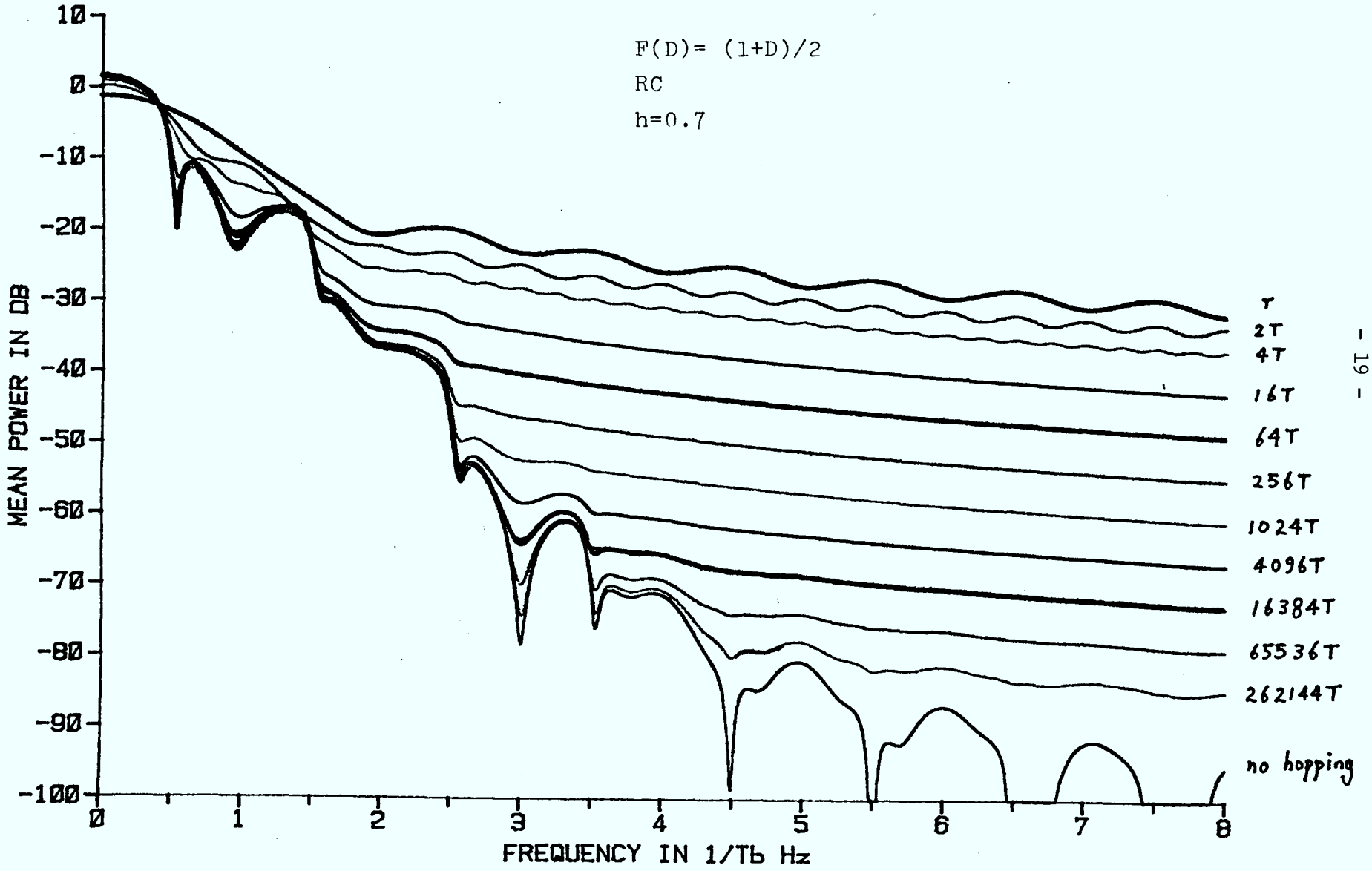

Fig.9 Hopped Duobinary FSK, h=0.7 with raised cosine pulse shaping

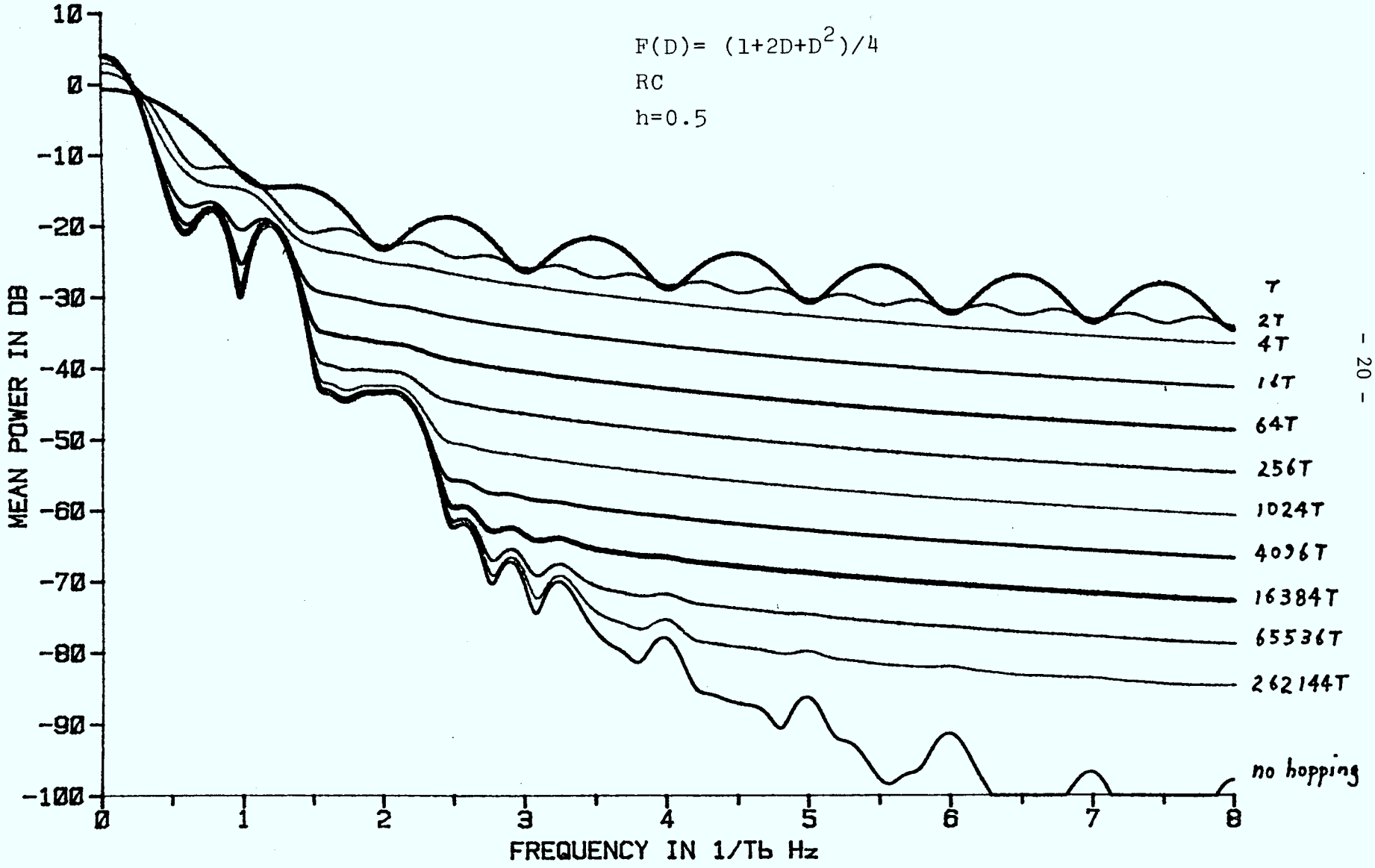

Fig.10 Hopped Tamed FM, h=0.5 with raised cosine pulse shaping

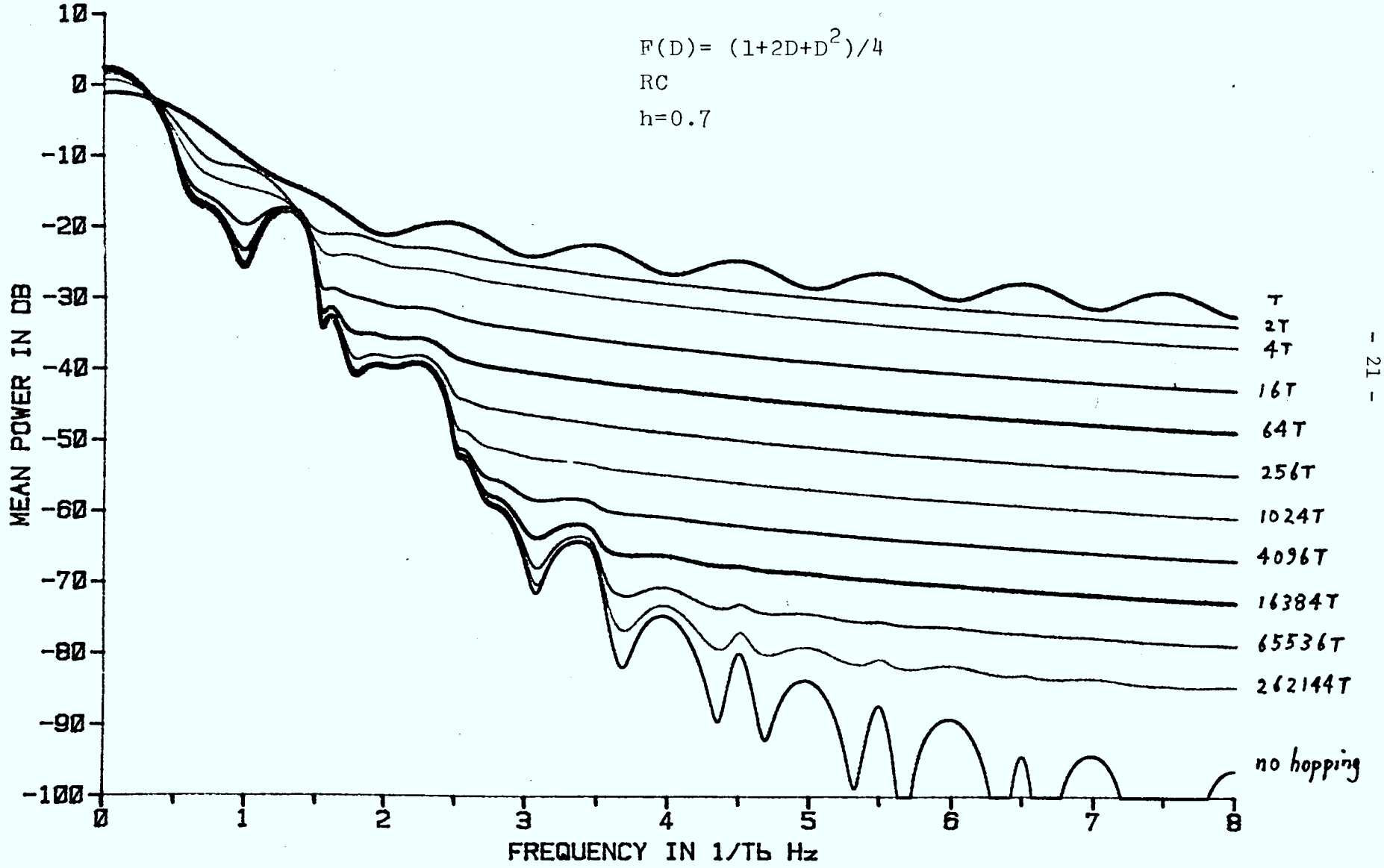

Fig.11 Hopped Tamed FM, h=0.7 with raised cosine pulse shaping

and $R_{CPM}(t,t+aT+\tau')$ is given by Eq.(2.14). The power density spectrum of the dehopped modulated signal is then obtained via a Fast Fourier Transform of the autocorrelation function of the signal, $R_u(\tau)$.

2.3 DISCUSSION

The power density spectra of the dehopped modulated signals with various partial response encodings together with different baseband pulse shaping have been calculated. The power density spectra for dehopped MSK for different lengths of hop interval are shown in Fig.2. As the length of the hop interval increases, the power density spectrum of the dehopped signal becomes more compact and the spectrum approaches that of coherent MSK without frequency hopping. The spectrum of the dehopped MSK is almost identical to the spectrum of coherent MSK for hop intervals of length greater than 2048 T.

With a modulation index of 0.7 and no correlative encoding, the spectrum of hopped CPFSK is as shown in Fig.3. If a comparison is made with the spectrum of MSK which has a modulation index of 0.5, we see that a change in the modulation index from 0.5 to 0.7 changes the shape of the spectrum quite significantly especially for short hop intervals. There are large side lobes when the length of the hop interval is equal to the transmitted symbol interval T.

To see the effect of correlative encoding on the hopped signal spectrum, the spectra for duobinary MSK are shown in Fig.4. Again the bandwidth occupied by the frequency-hopped signal reduces as the length of the hop interval increases, and the spectrum approaches that of coherent duobinary MSK as the length of the hop interval becomes

large. If the spectra are compared with MSK without correlative encoding, we notice that correlative encoding does not give much bandwidth reduction for short hop intervals. With long hop intervals it does. For the same duoboinary polynomial (1+D)/2, but a higher modulation index of 0.7, the spectra for the different hop lengths are as shown in Fig. 5. The signal bandwidth increases with an increase in modulation index when the length of the hop interval is large. To see if a higher order encoding polynomial would give a further improvement in the spectral characteristic, spectra for the Tamed FM (TFM) polynomial, which for coherent signaling is known to be an attractive second order PRS polynomial, were calculated as shown in Fig.6. A comparison of Fig. 6 and Fig. 2, shows that even for a higher order polynomial the reduction in bandwidth is insignificant at short hop intervals. However, for long hop intervals the higher order PRS polynomial yields a spectrum of even greater compactness with very low sidelobes.

To illustrate the effects of baseband pulse shaping on the spectra, the spectra for raised cosine pulse shaping with various encoding polynomials are as shown in Figs.8 to 11. For long hop lengths the spectra of the signals with raised cosine shaping are more compact than their rectangularly shaped counterparts.

From these results we conclude that the spectrum becomes more compact as the hop interval lengthens and in general approaches that of the CPM signal without hopping. An increase in the modulation index will increase the bandwidth occupied by the signal for long hop lengths. For short hop lengths the increase in bandwidth due to an increase in modulation index is not significant. Although it is well

known that correlative encoding and raised cosine baseband pulse shaping reduce the signal bandwidth and sidelobe level for conventional continuous phase modulation, for frequency-hopped signals with short hop interval lengths these techniques do not yield much reduction in bandwidth. Substantial spectral improvement with these methods can be achieved at the longer hop intervals.

3.NONCOHERENT RECEIVER

3.1 INTRODUCTION

Since the phase continuity of a CPM signal is not preserved from one hop to the next and the initial carrier phase at the beginning of each hop is unknown, noncoherent detection has to be used. Osborne and Luntz [7] and also Schonhoff [8] have derived the noncoherent maximum likelihood receiver for CPFSK yielding symbol-by-symbol decisions. The receiver observes 2n+1 bits of a CPFSK signal and decides on the $(n+1)^{st}$ or middle bit. Svensson and Sundberg [9] have generalized the detection algorithm to allow the decision symbol to be anywhere in the observation interval rather than just in the middle of the observation interval and to include partially coherent detection, which allows the error in the estimated carrier phase to have a nonuniform probability density function between $-\pi$ and π. Noncoherent symbol-by-symbol detection of correlative encoded CPM is also reported in [10] and [11]. It has been observed that the symbol decisions ought to be based on the entire received sequence [12]. For the slow frequency-hopped correlative encoded CPM signal, a noncoherent maximum likelihood sequence estimation (MLSE) receiver could be derived where the observation interval is the entire transmission period. However for simplicity and to gain insight into the problem, we will first study the receiver that carries out an optimum detection over each hop interval.

3.2 OPTIMUM NONCOHERENT HOP-BY-HOP DETECTION

The received dehopped signal can be represented by

$$r(t) = (2E/T)^{1/2} \sum_{i=-\infty}^{\infty} p(t-iNT)\cos[2\pi f_c t + \psi(t,\underline{\alpha}) + \theta_i] + n(t) \qquad (3.1)$$

where E is the symbol energy,

f_c is the carrier frequency,

n(t) is additive white Gaussian noise with double-sided power spectral density of No/2 W/Hz. The other symbols and notation are as defined and used previously.

Consider first a transmitted sequence $\underline{\alpha}$ of length n, which is less than or equal to N. Suppose the sequence lays in a single hop interval $0 < t < NT$. The initial random phase would then be constant over the transmission period. Let the dehopped transmitted signal over (0,nT), be denoted by $s(t,\underline{\alpha},\theta_o)$, where θ_o is the random phase due to the hop. The phase is assumed uniformly distributed over $(0,2\pi)$. The detector must now find the sequence of data symbols $\underline{\alpha}'$, which maximizes the likelihood function

$$\ell(\underline{\alpha},\underline{\alpha}') = E_{\theta_o}\{ \exp[(2a/N_o) \int_0^{nT} r(t)s(t,\underline{\alpha}',\theta_o)\, dt] \} \qquad (3.2)$$

where $a=(2E/T)^{1/2}$, n is the length of the transmitted sequence and $E_{\theta_o}\{\ \}$ denotes the mathematical expectation with respect to the random variable θ_o. The likelihood function is then given by

$$\ell(\underline{\alpha},\underline{\alpha}') = I_o\{(2a/N_o)\ [\ell_c^{\,2}(\underline{\alpha},\underline{\alpha}') + \ell_s^{\,2}(\underline{\alpha},\underline{\alpha}')\ ]^{1/2}\ \} \qquad (3.3)$$

where $I_o\{\ \}$ is the zeroth-order modified Bessel function, and

$$\ell_c(\underline{\alpha},\underline{\alpha}') = \int_0^{nT} r(t)\cos[2\pi f_c t + \psi(t,\underline{\alpha}')]dt \tag{3.4a}$$

$$\ell_s(\underline{\alpha},\underline{\alpha}') = \int_0^{nT} r(t)\sin[2\pi f_c t + \psi(t,\underline{\alpha}')]dt \tag{3.4b}$$

Since the Bessel function $I_o\{\ \}$ is a monotone increasing function, an equivalent likelihood function can simply be

$$\ell'(\underline{\alpha},\underline{\alpha}') = \ell_c^{\,2}(\underline{\alpha},\underline{\alpha}') + \ell_s^{\,2}(\underline{\alpha},\underline{\alpha}') \tag{3.5}$$

A brute force method of finding the most likely transmitted signal is to correlate the received signal with the inphase and quadrature components of all possible transmitted waveforms and to choose the transmitted sequence which gives the largest likelihood. However, this approach would be highly impractical considering the large number of correlators or matched filters required, particularly when the length of the transmitted sequence is large.

3.3 MAXIMUM LIKELIHOOD SEQUENCE ESTIMATION (MLSE)

For coherent detection, the Viterbi Algorithm, which was originally proposed for decoding convolutional codes, has been used for estimating the maximum likelihood sequence by calculating the likelihood recursively [13-16]. Since the likelihood for noncoherent detection as given by Eq.(3.5) is the sum of the square of the inphase correlator output and the square of the quadrature correlator output, the metric calculation is not as straightforward as in the coherent case.

To derive a recursive maximum-likelihood decoding algorithm, we

note that $\ell_c(\underline{\alpha},\underline{\alpha}')$ and $\ell_s(\underline{\alpha},\underline{\alpha}')$ given by Eq.(3.4) can be written as the sum of the partial likelihoods as

$$\ell_c(\underline{\alpha},\underline{\alpha}') = \sum_{k=0}^{n-1} \int_{kT}^{(k+1)T} r(t)\cos[2\pi f_c t + \psi(t,\underline{\alpha}')]\, dt \tag{3.6a}$$

$$\ell_s(\underline{\alpha},\underline{\alpha}') = \sum_{k=0}^{n-1} \int_{kT}^{(k+1)T} r(t)\sin[2\pi f_c t + \psi(t,\underline{\alpha}')]\, dt \tag{3.6b}$$

which are simply the sum of the appropriate inphase and quadrature correlator (or matched filter) outputs respectively.

The information carrying phase during the k^{th} symbol interval can be written as

$$\psi(t) = 2\pi h \sum_{n=k-L+1}^{k} \alpha_n\, q(t-nT) + 2\pi h \sum_{n=0}^{k-L} \alpha_n\, q(LT) \tag{3.7}$$

$$\text{for } kT < t < (k+1)T$$

The first term represents the contribution of inputs actively affecting the shape of the phase path during the k^{th} interval. For a given correlative encoder with PRS polynomial F(D) of degree m, the state can be defined by the latest m, or L-1 input digits. A correlative state vector can be defined as

$$C_k = [\alpha_{k-L+1}, \cdots\cdots, \alpha_{k-2}, \alpha_{k-1}] \tag{3.8}$$

The second term in (3.7) represents the underlying phase due to past inputs, which can be called the phase state [14]

$$\phi_k = \left[\, 2\pi h \sum_{n=0}^{k-L} \alpha_n\, q(LT) \,\right]_{\text{mod } 2\pi} \tag{3.9}$$

The combined state $s_k \triangleq [C_k, \phi_k]$, that is, the correlative state

vector and the phase state, together with the present input α_k, completely specify the transmitted signal waveform during the k^{th} interval.

If $h=2\ell/p$ for ℓ and p relatively prime integers, there are at most p possible distinct phase states $(0, 2\pi/p, 4\pi/p, \ldots, 2\pi(p-1)/p)$. For M-ary transmission there will then be $\mu=M^m$ different correlative states and p phase states for a total of $\eta=p\mu$ combined states at the most. Since the mapping of the input data sequence to the state sequence is one-to-one, estimation of the state sequence will given the corresponding estimated transmitted data sequence.

The maximum-likelihood decoding algorithm proceeds as follows. Starting from a known initial state $s_0 = i$, the decoder stores the inphase and quadrature likelihoods of the node $s_1 = j$ as

$$\ell^*_{c,1}(j) = \delta_c(i,j) \tag{3.10a}$$

$$\ell^*_{s,1}(j) = \delta_s(i,j) \tag{3.10b}$$

$$\text{for } j=1,2,\ldots,\eta$$

where $\delta_c(i,j)$ and $\delta_s(i,j)$ are just the appropriate inphase and quadrature matched filter outputs corresponding to the partial likelihoods in Eq.(3.6) for the transition from the node i to the node j during a symbol interval.

In general at time $k(\geq 2)$, the decoder compares for each node $s_k=j$ the likelihood functions of the η different paths leading to $s_k=j$, i.e.

$$\ell'_k(j) = [\ell^*_{c,k-1}(i) + \delta_c(i,j)]^2 + [\ell^*_{s,k-1}(i) + \delta_s(i,j)]^2 \tag{3.11}$$

$$i=1,2,\ldots,\eta$$

Let the path with the largest likelihood function be called the

survivor, since only this branch has the possibility of being a portion of the maximum-likelihood path and hence should be preserved. Other $\eta-1$ paths ending at $s_k=j$ can be discarded.

Thus the metric of the survivor at $s_k=j$ is

$$\ell^*_k(j) = \max_i \{[\ell^*_{c,k-1}(i) + \delta_c(i,j)]^2 + [\ell^*_{s,k-1}(i) + \delta_s(i,j)]^2\} \tag{3.12}$$

where $j = 1,2,\ldots,\eta$ and $k \geq 2$.

While $\ell^*_k(j)$ is defined as the metric of the node $s_k=j$ at time k, the pair $(\ell^*_{c,k}(j), \ell^*_{s,k}(j))$ are stored for node $s_k=j$, as given by

$$\ell^*_{c,k}(j) = \ell^*_{c,k-1} + \delta_c(i,j) \tag{3.13a}$$

$$\ell^*_{s,k}(j) = \ell^*_{s,k-1} + \delta_s(i,j) \tag{3.13b}$$

where i is the node index satisfying Eq.(3.12). The metric is computed sequentially from the old information $(\ell^*_{c,k-1}(j), \ell^*_{s,k-1}(j))$ and the matched filter outputs $(\delta_c(i,j), \delta_s(i,j))$ in the k^{th} interval according to Eq.(3.12). The maximum likelihood decoding algorithm now has to accumulate both the inphase and quadrature likelihood parameters rather than just the inphase likelihood parameter as in the coherent case.

We do not know the true state s_k at time k, but we do know that it must be one of the finite number of states j, $1 \leq j \leq \eta$. Consequently, while we cannot make a final decision as to the identity of the initial segment of the maximum-likelihood state sequence at time k, we know that the initial segment must be among the η survivors $\underline{s}_j$, $1 \leq j \leq \eta$, one for each state j.

In principle the algorithm can make a final decision on the initial state segment up to time (k-1)T when and only when all survi-

vors at time kT have the same initial state sequence segment up to time (k-1)T. That is, all surviving paths branch out from a common node, say $s_{k-1}=j$. The initial segment of the maximum-likelihood path is then uniquely determined independent of succeeding observation and a firm decision is available from the algorithhm. The decoding delay d is unbounded but is generally finite with probability 1 [12].

3.4 RECEIVER STRUCTURE

The noncoherent receiver must be able to provide the inphase and quadrature correlations of the received signal with every possible duration-T signal segment as indicated by Eq.(3.6). The inphase correlation over the k^{th} symbol interval required for the possible transition from node i to node j during the k^{th} symbol interval is given by

$$\delta_c(i,j) = \int_{kT}^{(k+1)T} r(t)\cos[2\pi f_c t + \psi(t,\underline{\alpha}')]\, dt$$

$$= \int_{kT}^{(k+1)T} r_c(t)\cos\,\psi(t,\underline{\alpha}')dt - \int_{kT}^{(k+1)T} r_s(t)\,\sin\,\psi(t,\underline{\alpha}')dt \qquad (3.14)$$

where $$r_c(t) = r(t)\cos 2\pi f_c t \qquad (3.15)$$

$$r_s(t) = r(t)\sin 2\pi f_c t \qquad (3.16)$$

The information carrying phase function $\psi(t,\underline{\alpha})$ during the k^{th} symbol interval as given by Eq. (3.7) can be written as

$$\psi(t,\underline{\alpha}') = \beta_{ki}(t) + \phi_{ki} \qquad kT < t < (k+1)T \qquad (3.17)$$

where $$\beta_{ki}(t) = 2\pi h \sum_{n=k-L+1}^{k} \alpha_n\, q(t-nT) \qquad (3.18)$$

$\beta_{ki}(t)$ is one of the M^L posible phase paths and ϕ_{ki} is one of the p possible phase states as given by Eq.(3.9). Substituting Eq.(3.17) into (3.14), we obtain

$$\begin{aligned}\delta_c(i,j) = &\cos\phi_{ki}\int_{kT}^{(k+1)T} r_c(t)\cos\beta_{ki}(t)dt \\ &- \sin\phi_{ki}\int_{kT}^{(k+1)T} r_c(t)\sin\beta_{ki}(t)dt \\ &- \cos\phi_{ki}\int_{kT}^{(k+1)T} r_s(t)\sin\beta_{ki}(t)dt \\ &- \sin\phi_{ki}\int_{kT}^{(k+1)T} r_s(t)\cos\beta_{ki}(t)dt \qquad (3.19)\end{aligned}$$

Similarly, the quadrature correlation over the k^{th} symbol interval for the transition from node i to node j is given by

$$\begin{aligned}\delta_s(i,j) = &\sin\phi_{ki}\int_{kT}^{(k+1)T} r_c(t)\cos\beta_{ki}(t)dt \\ &+ \cos\phi_{ki}\int_{kT}^{(k+1)T} r_c(t)\sin\beta_{ki}(t)dt \\ &- \sin\phi_{ki}\int_{kT}^{(k+1)T} r_s(t)\sin\beta_{ki}(t)dt \\ &+ \cos\phi_{ki}\int_{kT}^{(k+1)T} r_s(t)\cos\beta_{ki}(t)dt \qquad (3.20)\end{aligned}$$

where $r_c(t)$ and $r_s(t)$ are given by Eqs.(3.15) and (3.16), which are obtained by multiplying the received signal by $\cos 2\pi f_c t$ and $\sin 2\pi f_c t$ to form quadrature channels. A baseband matched filter bank is required to provide the correlations with the cosine and sine of all posible phase paths $\beta_{ki}(t)$ over each symbol interval to obtain the $\delta_c(i,j)$ and $\delta_s(i,j)$ required by the decoder. Notice that $\delta_c(i,j)$ and

$\delta_s(i,j)$ given by Eqs.(3.19) and (3.20) can share the same matched filter bank, since the difference is only in the scaling multipliers, $\sin \phi_{ki}$ and $\cos \phi_{ki}$ and the sign.

The matched filter impulse response is simply

$$\begin{aligned} hc_i &= \cos[\beta_{ki}(T-t)] && 0 < t < T, \\ &= 0 && \text{elsewhere.} \\ &= \cos 2\pi h \sum_{\ell=-L+1}^{0} \alpha_{i\ell}\, q[(1-\ell)T-t] && 0 < t < T, \\ &= 0 && \text{elsewhere.} \end{aligned} \tag{3.21}$$

to provide the correlation with the cosine of the i^{th} possible phase path. For the correlation with the sine of the i^{th} possible phase path, the impulse reponse of the required matched filter is given by

$$\begin{aligned} hs_i(t) &= \sin[\beta_{ki}(T-t)] && o < t < T, \\ &= 0 && \text{elsewhere.} \\ &= \sin 2\pi h \sum_{\ell=-L+1}^{0} \alpha_{i\ell}\, q[(1-\ell)T-t] && o < t < T, \\ &= 0 && \text{elsewhere.} \end{aligned} \tag{3.22}$$

There are, at the most, M^L possible distinct phase paths $\beta_{ki}(t)$. Hence the number of matched filters required is $4M^L$ at most. The number of matched filters can be reduced by a factor of two by noting that for every digit sequence, there is another sequence with opposite signs. Therefore, at the most, $2M^L$ baseband matched filters are required in total. A block diagram for the MLSE noncoherent receiver is shown in Fig.12.

The matched filter outputs are sampled every T seconds to obtain the inphase and quadrature correlations $\delta_c(i,j)$ and $\delta_s(i,j)$ for the

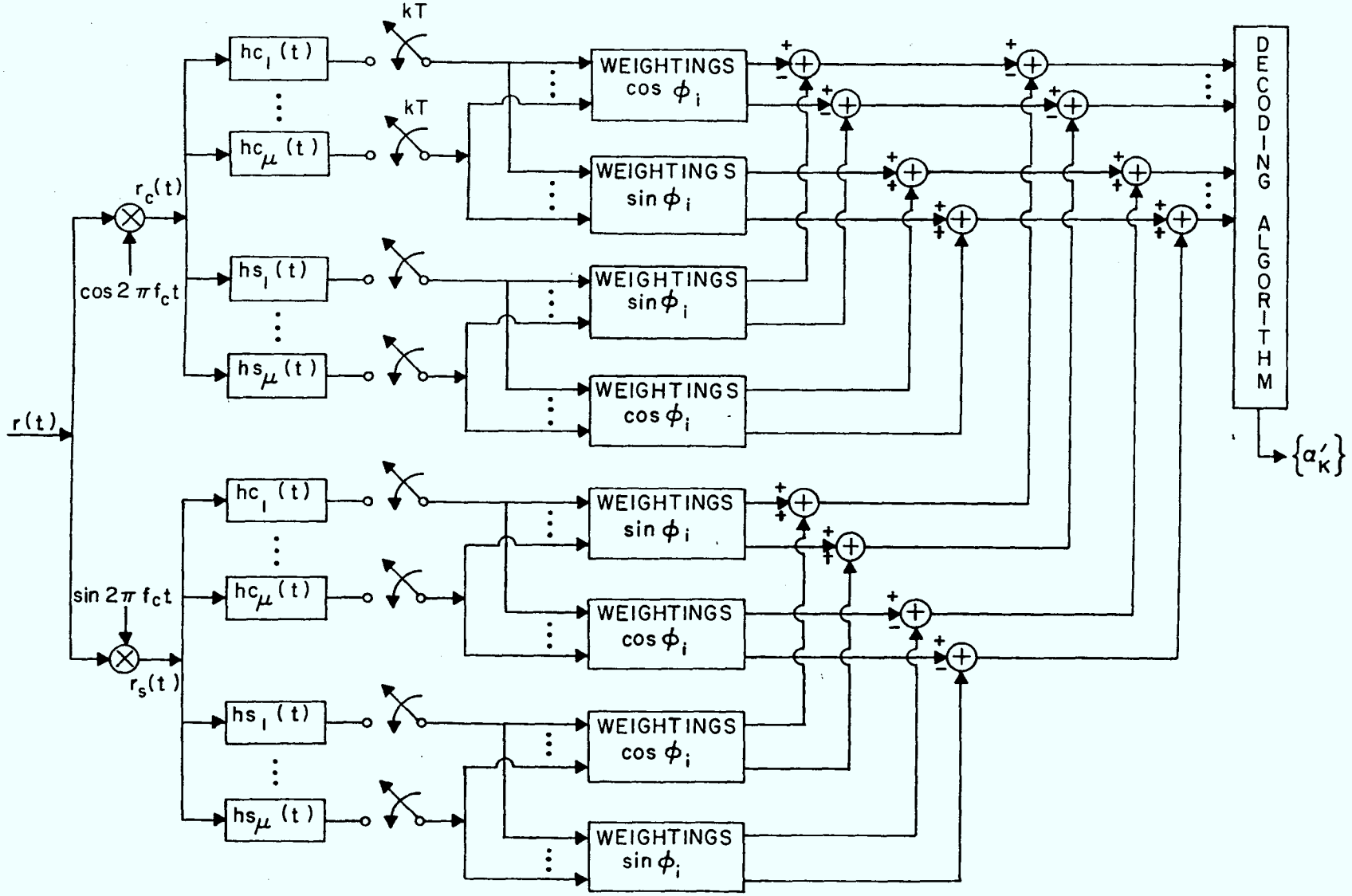

Fig. 12 NONCOHERENT MLSE RECEIVER BLOCK DIAGRAM

k^{th} symbol interval. There will be $\eta = pM^m = pM^{L-1}$ combined states per interval at most. Hence the decoding algorithm requires 2η storage locations for storing the inphase and quadrature likelihoods $\ell^*_{c,k-1}(i)$ and $\ell^*_{s,k-1}(i)$, $1 \leq i \leq \eta$. At each time kT, the algorithm has to perform $2M\eta$ additions to find $[\ell^*_{c,k-1}(i) + \delta_c(i,j)]$ and $[\ell^*_{s,k-1}(i) + \delta_s(i,j)]$ followed by $2M\eta$ squaring operations and $M\eta$ additions to obtain the likelihood $\ell'(\underline{\alpha},\underline{\alpha}')$. $(M-1)\eta$ binary comparisons are then required to determine the η survivors $\underline{S}_j$, $1 \leq j \leq \eta$ with the largest likelihood $\ell^*_k(j)$, $1 \leq j \leq \eta$. Hence, at each time kT, a total of $3pM^L$ additions and $2pM^L$ squaring operations and $(M-1)pM^{L-1}$ binary comparisons are performed by the decoder.

3.4.1 Matched Filters

In this section further detail on the matched filters is presented. Recall that the impulse response of the matched filters is given as follows.

$$hc_i(t) = \cos[\beta_i(T-t)] \qquad 0 < t \; T,$$

$$= 0 \qquad \text{elsewhere.}$$

$$= \cos 2\pi h \sum_{\ell=-L+1}^{0} \alpha_{i\ell} q[(1-\ell)T-t] \qquad 0 < t < T,$$

$$= 0 \qquad \text{elsewhere.}$$

$$hs_i(t) = \sin[\beta_i(T-t)] \qquad 0 < t < T,$$

$$= 0 \qquad \text{elsewhere.}$$

$$= \sin 2\pi h \sum_{\ell=-L+1}^{0} \alpha_{i\ell} q[(1-\ell)T-t] \qquad 0 < t < T,$$

$= 0$ elsewhere.

(a)Filters for Duobinary MSK (DMSK)

The modulation index $h = 1/2$, and

$$q(t) = \begin{cases} 0 & t < 0 \\ \frac{t}{4T} & 0 < t < 2T \\ \frac{1}{2} & t > 2T \end{cases}$$

$$hc_i(t) = \cos \pi[\alpha_{io}\, q(T-t) + \alpha_{i-1}\, q(2T-t)]$$

$$= \cos \pi[\alpha_{io}\, (\frac{T-t}{4T}) + \alpha_{i-1}\, (\frac{2T-t}{4T})]$$

$$= \cos \frac{\pi}{4T}\, [\alpha_{io}(T-t) + \alpha_{i-1}(2T-t)]$$

α_{io} and α_{i-1} can take on values of +1 and -1 for binary transmission. Hence there are at most $2^2 = 4$ possible cosine filters with $hc_i(t)$ given by

$$hc_1(t) = \cos \frac{\pi}{4T}\, [(T-t) + (2T-t)] = \cos \frac{\pi}{4T}\, (3T-2t) = \cos \frac{\pi}{4T}\, [2t-3T]$$

$$hc_2(t) = \cos \frac{\pi}{4T}\, [(T-t) - (2T-t)] = \cos (-\frac{\pi}{4}) = \cos \frac{\pi}{4}$$

$$hc_3(t) = \cos \frac{\pi}{4}\, \{-(T-t) + (2T-t)] = \cos (\frac{\pi}{4}) = hc_2(t)$$

$$hc_4(t) = \cos \frac{\pi}{4T}\, [-(T-t) - (2T-t)] = \cos \frac{\pi}{4T}\, [-3T+2t]$$

$$= \cos \frac{\pi}{4T}\, [2t-3T] = hc_1(t)$$

Matched filter hc_1 is the same as hc_4, and hc_2 is the same as hc_3. Thus only two filters are required for each of the inphase and quadrature arms. The matched filters for the sine correlations are

$$hs_i(t) = \sin \frac{\pi}{4T} [\alpha_{io}(T-t) + \alpha_{i-1}(2T-t)]$$

Hence

$$hs_1(t) = \sin \frac{\pi}{4T} [(T-t) + (2T-t)] = \sin \frac{\pi}{4T} (3T-2t)$$

$$hs_2(t) = \sin \frac{\pi}{4T} [(T-t) - (2T-t)] = \sin \frac{\pi}{4T} [-T] = - \sin \frac{\pi}{4}$$

$$hs_3(t) = \sin \frac{\pi}{4T} [-(T-t) + (2T-t)] = \sin \frac{\pi}{4} = - hs_2(t)$$

$$hs_4(t) = \sin \frac{\pi}{4T} [-(T-t) - (2T-t)] = \sin \frac{\pi}{4T} (-3T+2t) = - hs_1(t)$$

Again only two distinct filters $hs_1(t)$ and $hs_2(t)$ are required for each of the inphase and quadrature arms, or a total of four filters. Thus the total number of matched filters required is eight. Note that $hc_2(t) = \cos \pi/4$, and $hs_2(t) = -\sin \pi/4$, are just scaling integrate-and-dump filters.

(b)Filters for Tamed FM (TFM)

We now present the matched filters required for reception of Tamed FM.

$$hc_i(t) = \cos 2\pi h\{\alpha_{io}\, q(T-t) + \alpha_{i-1}\, q(2T-t) + \alpha_{i-2}\, q(3T-t)\}$$

$$= \cos 2\pi h\{\alpha_{io}(\frac{1}{8} - \frac{t}{8T}) + \alpha_{i-1}(\frac{3}{8} - \frac{t}{4T}) + \alpha_{i-2}(\frac{1}{2} - \frac{t}{8T})\}$$

$$hc_1(t) = \cos 2\pi h\{\frac{1}{8} - \frac{t}{8T} + \frac{3}{8} - \frac{t}{4T} + \frac{1}{2} - \frac{t}{8T}\}$$

$$= \cos 2\pi h[1 - \frac{t}{2T}] \qquad (1)$$

$$hc_2(t) = \cos\ 2\pi h\{\frac{1}{8} - \frac{t}{8T} + \frac{3}{8} - \frac{t}{4T} - \frac{1}{2} + \frac{t}{8T}\}$$

$$= \cos\ 2\pi h\ [-\frac{t}{4T}]$$

$$= \cos\ \frac{\pi h}{2T}\ t \qquad (2)$$

$$hc_3(t) = \cos\ 2\pi h\{\frac{1}{8} - \frac{t}{8T} - \frac{3}{8} + \frac{t}{4T} + \frac{1}{2} - \frac{t}{8T}\}$$

$$= \cos\ 2\pi h\{\frac{1}{4}\}$$

$$= \cos\ \frac{\pi h}{2} \qquad (3)$$

$$hc_4(t) = \cos\ 2\pi h\ \{\frac{1}{8} - \frac{t}{8T} - \frac{3}{8} + \frac{t}{4T} - \frac{1}{2} + \frac{t}{8T}\}$$

$$= \cos\ 2\pi h\{-\frac{3}{4} + \frac{t}{4T}\} \qquad (4)$$

$$hc_5(t) = \cos\ 2\pi h\{-\frac{1}{8} + \frac{t}{8T} + \frac{3}{8} - \frac{t}{4T} + \frac{1}{2} - \frac{t}{8T}\}$$

$$= \cos\ 2\pi h\{\frac{3}{4} - \frac{t}{4T}\}$$

$$= hc_4(t)$$

$$hc_6(t) = hc_3(t)$$

$$hc_7(t) = hc_2(t)$$

$$hc_8(t) = hc_1(t)$$

Hence there appear to be 4 $hc_i(t)$'s given by Eqs. (1) to (4), required.

$$hs_1(t) = \sin\ 2\pi h\{1 - \frac{t}{2T}\} \qquad (5)$$

$$hs_2(t) = \sin\ 2\pi h\{-\frac{t}{4T}\} \qquad (6)$$

$$hs_3(t) = \sin\ (\pi h/2) \qquad (7)$$

$$hs_4(t) = \sin 2\pi h\{-\frac{3}{4} + \frac{t}{4T}\} \qquad (8)$$

$$hs_5(t) = -hs_4(t)$$

$$hs_6(t) = -hs_3(t)$$

$$hs_7(t) = -hs_2(t)$$

$$hs_8(t) = -hs_1(t)$$

Each of the distinct matched filters hc_i and hs_i must be implemented in each of the inphase and quadrature arms. Hence it would first appear that the total number of matched filters required for the Tamed FM receiver is 16. However the response of hc_4 and hs_4 can be obtained by scaling and adding the responses of hc_2, hc_3, hs_2, and hs_3 and the number of matched filters required is only 12.
Note that $hc_3(t) = \cos \pi h/2$, and $hs_3(t) = \sin \pi h/2$, are just scaling integrate-and-dump filters.

3.5 ERROR PERFORMANCE ANALYSIS OF THE OPTIMUM HOP-BY-HOP RECEIVER

Given that the sequence $\underline{\alpha}_n = \{\alpha_0, \alpha_1, \alpha_2, \ldots, \alpha_{n-1}\}$ is transmitted, a sequence error occurs whenever the estimated sequence $\underline{\alpha}'_n = \{\alpha'_0, \alpha'_1, \alpha'_2, \ldots, \alpha'_{n-1}\}$ is different from $\underline{\alpha}_n$ in one or more places. Over a long time the estimated path and the correct path will typically diverge and remerge a number of times. Each distinct separation is called an error event [12,13]. The set ε_{k_1} of all possible error events starting at some time k_1 is a tree-like trellis which starts at

S_{k_1} and each of whose branches ends on the correct path. For the MLSE receiver described previously, a firm decision on the estimated sequence $\underline{\alpha}$ will be available as soon as a merge has occurred. Hence, the probability of any particular error event $\underline{\alpha}'_{k_2}$, starting at time k_1T and ending at time k_2T is simply the probability that the observation over the interval 0 to k_2T, $\underline{\alpha}'_{k_2}$, is more likely than $\underline{\alpha}_{k_2}$.

The probability of any particular error event E is then simply given by

$$\Pr[E] = \Pr\{\ell'(\underline{\alpha}_{k_2}, \underline{\alpha}'_{k_2}) > \ell'(\underline{\alpha}_{k_2}, \underline{\alpha}_{k_2})\} \qquad (3.23)$$

$$\underline{\alpha}'_{k_2} \neq \underline{\alpha}_{k_2}$$

where

$$\ell'(\underline{\alpha}_{k_2}, \underline{\alpha}'_{k_2}) = \left(\int_0^{k_2T} r(t) \cos[2\pi f_c t + \psi(t, \underline{\alpha}')]dt \right)^2 + \left(\int_0^{k_2T} r(t) \sin[2\pi f_c t + \psi(t, \underline{\alpha}')]dt \right)^2 \qquad (3.24)$$

and

$$\ell'(\underline{\alpha}_{k_2}, \underline{\alpha}_{k_2}) = \left(\int_0^{k_2T} r(t) \cos[2\pi f_c t + \psi(t, \underline{\alpha})]dt \right)^2 + \left(\int_0^{k_2T} r(t) \sin[2\pi f_c t + \psi(t, \underline{\alpha})]dt \right)^2 \qquad (3.25)$$

where $\psi(t, \underline{\alpha})$ is the information carrying phase function given previously. Since the correlator references are the inphase and quadrature components of a constant amplitude waveform, $\ell'(\underline{\alpha}, \underline{\alpha}')$ may be regarded as the output of a complex correlator with reference $\bar{s}(t, \underline{\alpha}')$, which is given by

$$\bar{s}\ (t,\underline{\alpha}') = \cos\ [2\pi f_c t + \psi\ (t,\underline{\alpha}')] + j\ \sin\ [2\pi f_c t + \psi(t,\underline{\alpha}')]$$

$$= \exp\ j\ [2\pi f_c t + \psi(t,\underline{\alpha}')] \qquad (3.26)$$

The likelihood parameter $\ell'(\underline{\alpha},\underline{\alpha}')$ may be written in complex notation as

$$\ell'(\underline{\alpha},\underline{\alpha}') = \left| \int_0^{k_2 T} r(t)\ \exp\ j\ [2\pi f_c t + \psi(t,\underline{\alpha}')]\ dt \right|^2 = |Z_1|^2 \qquad (3.27)$$

Similarly, we have

$$\ell'(\underline{\alpha},\underline{\alpha}) = \left| \int_0^{k_2 T} r(t)\ \exp\ j\ [2\pi f_c t + \psi(t,\underline{\alpha})]\ dt \right|^2 = |Z_2|^2 \qquad (3.28)$$

Since

$$P_r[\ \ell'(\underline{\alpha},\underline{\alpha}') > \ell'(\underline{\alpha},\underline{\alpha})] = P_r[\ |Z_1| > |Z_2|\ ] \qquad (3.29)$$

the probability of an error event is just the probability of one Rician variable exceeding another and the solution is

$$P_r\ [E] = \frac{1}{2}\ [\ 1 - Q\ (\sqrt{b},\sqrt{a}\ ) + Q\ (\sqrt{a},\sqrt{b})] \qquad (3.30)$$

where Q ( ) is the Marcum Q function defined by

$$Q(x,y) = \int_y^{\infty} \exp\ (-\ \frac{x^2+u^2}{2}) \ I_o\ (xu)\ udu \qquad (3.31)$$

A recursive method for calculating the Marcum Q function is given in [18].

The parameters in Eq.(3.30) are given by

$$\begin{Bmatrix} a \\ b \end{Bmatrix} = \frac{1}{2\sigma^2}\ \left\{ \frac{|M_1|^2 + |M_2|^2 - 2R_e(M_1^* M_2 \rho)}{1 - |\rho|^2} \mp \frac{|M_2|^2 - |M_1|^2}{(1 - |\rho|^2)^{1/2}} \right\} \qquad (3.32)$$

The parameters in Eq. (3.32) are given by

$$M_1 = E\ \{Z_1\}$$

$$M_2 = E\ \{Z_2\}$$

$$\sigma^2 = Var\{Z_1\} = Var\{Z_2\} = E\ \{(Z_1 - M_1)^*(Z_1 - M_1)\} \qquad (3.33)$$

$$\rho = -\frac{1}{\sigma^2} E\{(Z_2 - M_2)^* (Z_1 - M_1)\}$$

where the expectation is taken with respect to the Gaussian channel noise. It can be shown that a and b are given by

$$\left\{\begin{matrix} a \\ b \end{matrix}\right\} = \frac{k_2 E_b}{2N_o} (\log_2 M) \left[1 \mp \{1 - |\rho(\underline{\alpha}, \underline{\alpha}')|^2\}^{1/2} \right] \qquad (3.34)$$

where $\rho(\underline{\alpha}, \underline{\alpha}')$ is the complex correlation between the two complex signals $\bar{s}(t, \underline{\alpha}')$ and $\bar{s}(t, \underline{\alpha})$. $|\rho(\underline{\alpha}, \underline{\alpha}')|^2$ is given by

$$|\rho(\underline{\alpha}, \underline{\alpha}')|^2 = \left| \frac{1}{k_2 T} \int_0^{k_2 T} \bar{s}(\underline{\alpha}, \underline{\alpha}') \bar{s}^*(\underline{\alpha}, \underline{\alpha}) \, dt \right|^2$$

$$= \left| \frac{1}{k_2 T} \int_0^{k_2 T} e^{j[2\pi f_c t + \psi(t, \underline{a}')]} e^{-j[2\pi f_c t + \psi(t, \alpha)]} \, dt \right|^2$$

$$= \left| \frac{1}{k_2 T} \int_0^{k_2 T} \exp j \, [\psi(t, \underline{\alpha}') - \psi(t, \underline{\alpha})] \, dt \right|^2$$

$$= \left(\frac{1}{k_2 T} \int_0^{k_2 T} \cos [\psi(t, \underline{\alpha}') - \psi(t, \underline{\alpha})] \, dt \right)^2$$

$$+ \left(\frac{1}{k_2 T} \int_0^{k_2 T} \sin [\psi(t, \underline{\alpha}') - \psi(t, \underline{\alpha})] \, dt \right)^2 \qquad (3.35)$$

Since $\psi(t, \underline{\alpha}') - \psi(t, \underline{\alpha}) = \psi(t, \underline{\alpha}' - \underline{\alpha})$, the complex correlation $\rho(\underline{\alpha}', \underline{\alpha})$ actually depends on the difference sequence $\underline{\gamma} = \underline{\alpha}' - \underline{\alpha}$ (3.36) rather than on both $\underline{\alpha}'$ and $\underline{\alpha}$. Eq. (3.35) can be rewritten as

$$|\rho(\underline{\alpha}', \underline{\alpha})|^2 = |\rho(\underline{\gamma})|^2$$
$$= \left(\frac{1}{k_2 T} \int_0^{k_2 T} \cos \psi(t, \underline{\gamma}) dt \right)^2 + \left(\frac{1}{k_2 T} \int_0^{k_2 T} \sin \psi(t, \underline{\gamma}) dt \right)^2 \quad (3.37)$$

For an error event starting at time $k_1 T$, $\psi(t, \underline{\gamma}) = 0$ for $t < k_1 T$, hence we have

$$|\rho(\underline{\gamma})|^2 = \left[\frac{1}{k_2 T} \left(k_1 T + \int_{k_1 T}^{k_2 T} \cos \psi(t, \underline{\gamma}) \, dt \right) \right]^2$$
$$+ \left[\frac{1}{k_2 T} \int_{k_1 T}^{k_2 T} \sin \psi(t, \underline{\gamma}) dt \right]^2 \quad (3.38)$$

The probability of any particular error event starting and ending at times $k_1 T$ and $k_2 T$ respectively can then be calculated using Eqs.(3.30), (3.34) and (3.38). It can be shown that error paths having the largest complex correlations $|\rho(\underline{\gamma})|$ will have the highest probability of occurrence. A quantity related to the Euclidean distance in coherent detection is the equivalent Euclidean distance, introduced as an error performance measure for the noncoherent receiver in [9],[10],[11]. Asymptotically, the equivalent Euclidean distance plays the same role as the Euclidean distance in the coherent case and it relates to the complex correlation through the following expression

$$d_e^2 = k_2 \, (1 - |\rho(\underline{\gamma})|) \log_2(M) \quad (3.39)$$

A set of the error events which start at time 0 and have the smallest equivalent distances, is first determined. The equivalent distances of the error signal paths associated with these error events starting at various times are then calculated. The equivalent dis-

tance results for MSK, DMSK and TFM with rectangular pulse shaping are shown in Figs.13 to 15.

As can be seen from these results, some error events have equivalent distances that stay constant independent of the starting time of the error event. If the error phase path $\psi(t,\underline{\gamma})$ has a particular shape over k_1T to k_2T such that

$$\int_{k_1T}^{k_2T} \sin \psi(t,\underline{\gamma})\, dt = 0 \tag{3.40}$$

then

$$|\rho(\underline{\gamma})|^2 = \left[\frac{1}{k_2T} (k_1T + \int_{k_1T}^{k_2T} \cos \psi(t,\underline{\gamma})\, dt)\right]^2 \tag{3.41}$$

and the equivalent distance for this particular error path is

$$d_e^2 = (k_2 - k_1) - \frac{1}{T} \int_{k_1T}^{k_2T} \cos \psi(t,\underline{\gamma})\, dt \tag{3.42}$$

For any error event which satisfies Eq.(3.40), d_e^2 will be independent of the starting time k_1T of the error event. This explains why some of the d_e^2 are constant independent of starting time.

The probability of each of these error events at a SNR of 10 dB is evaluated and plotted in Figs.16 to 18.

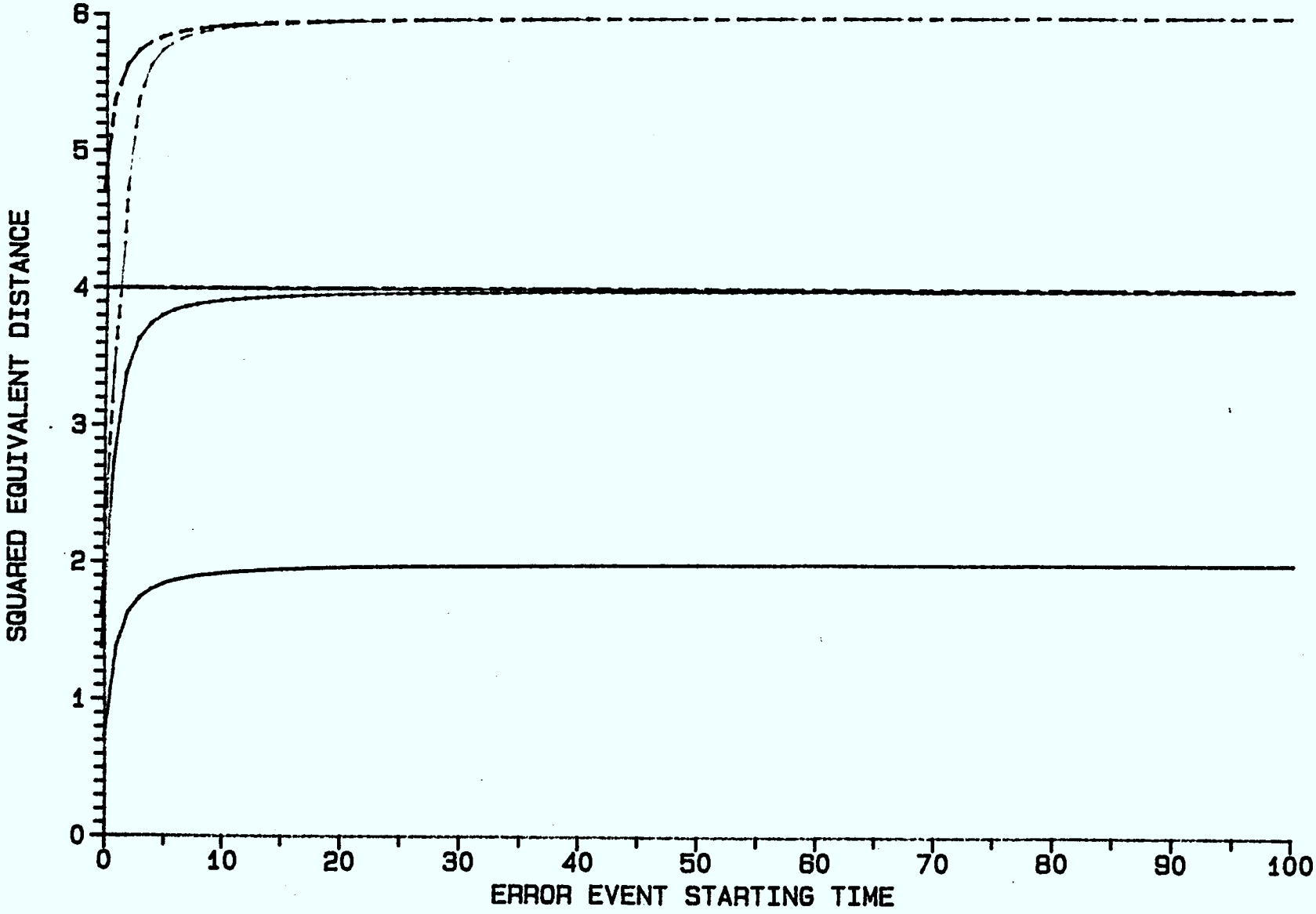

Fig. 13 d_e^2 for MSK

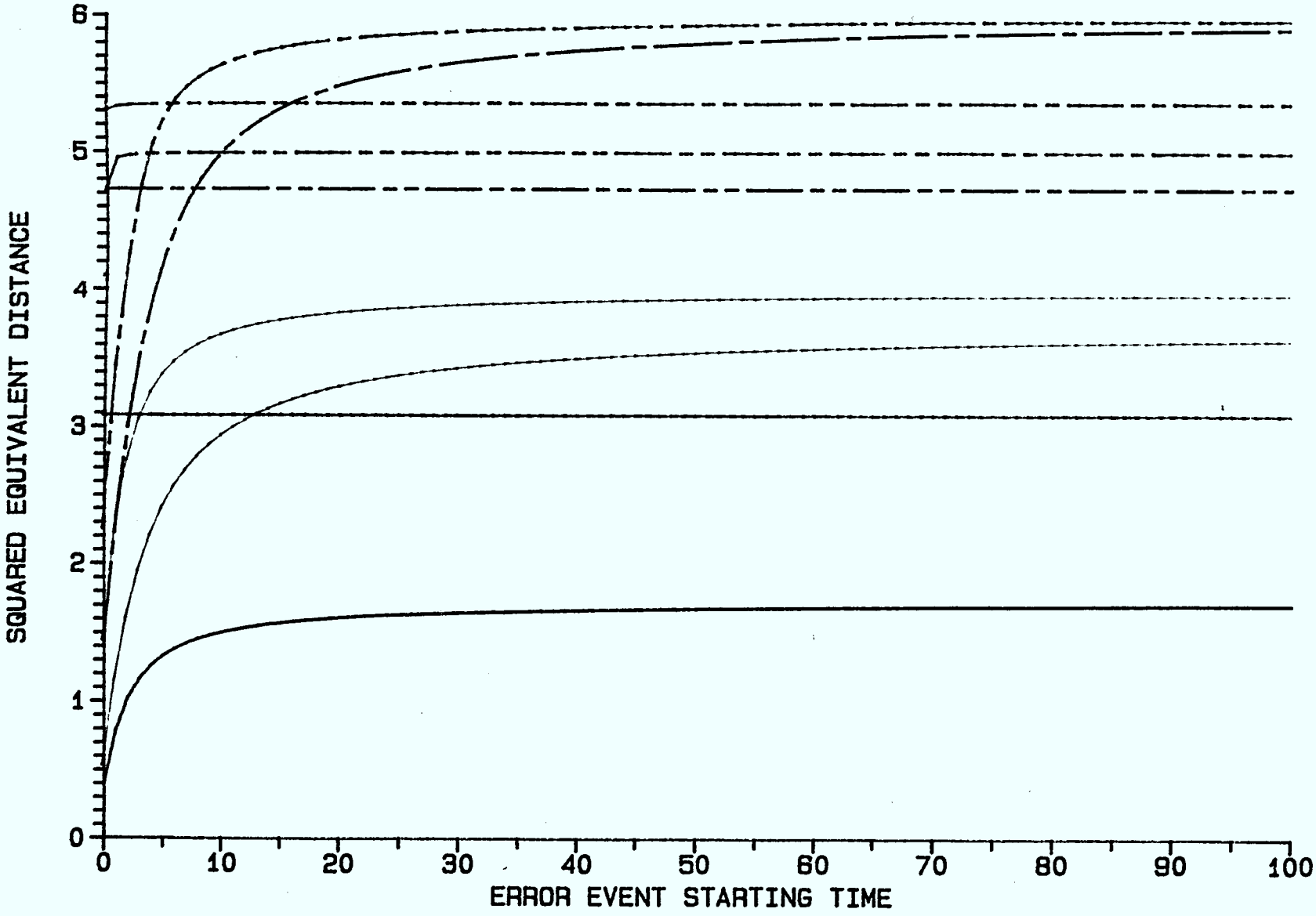

Fig. 14 d_e^2 for DMSK

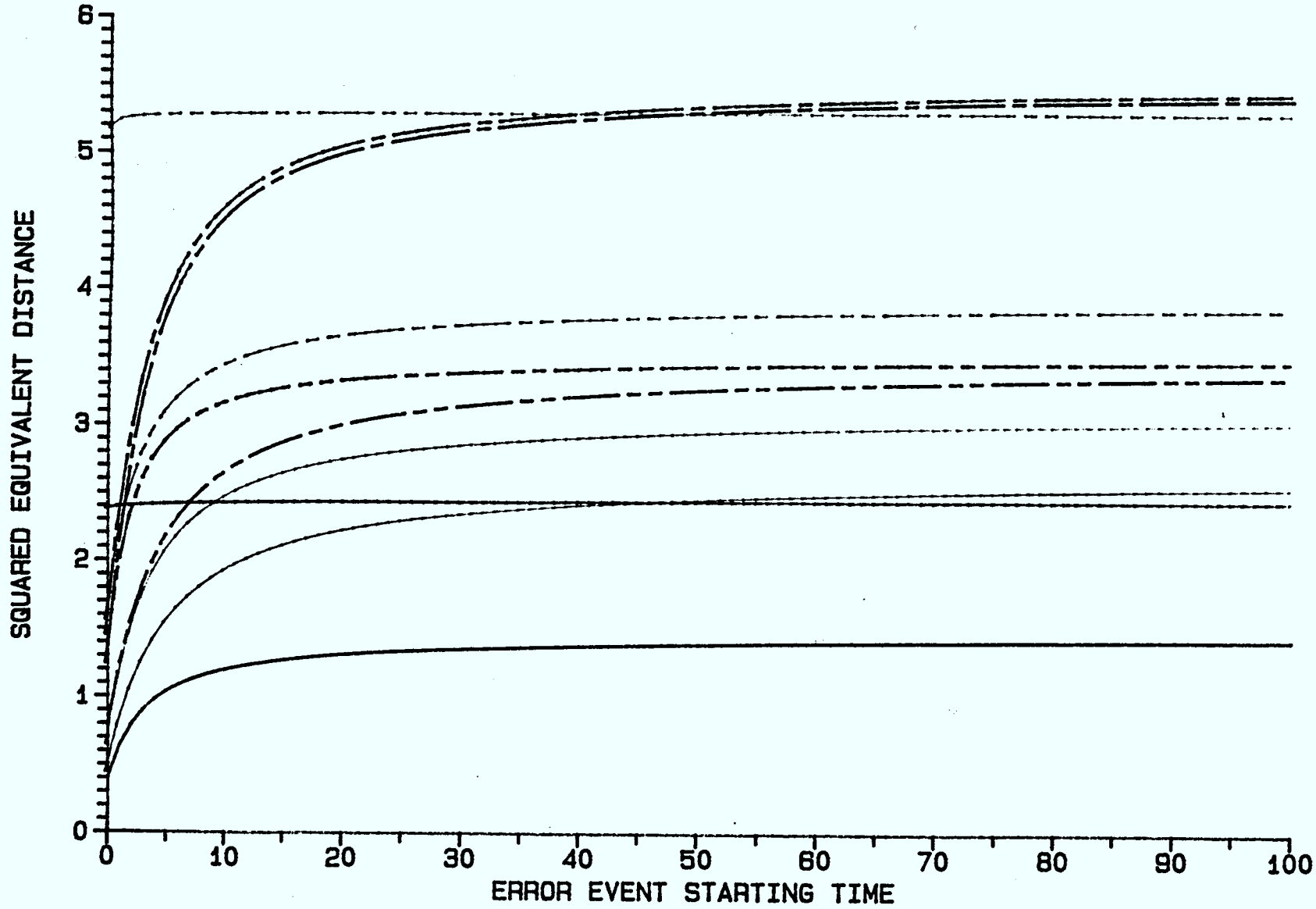

Fig. 15 d_e^2 for TFM

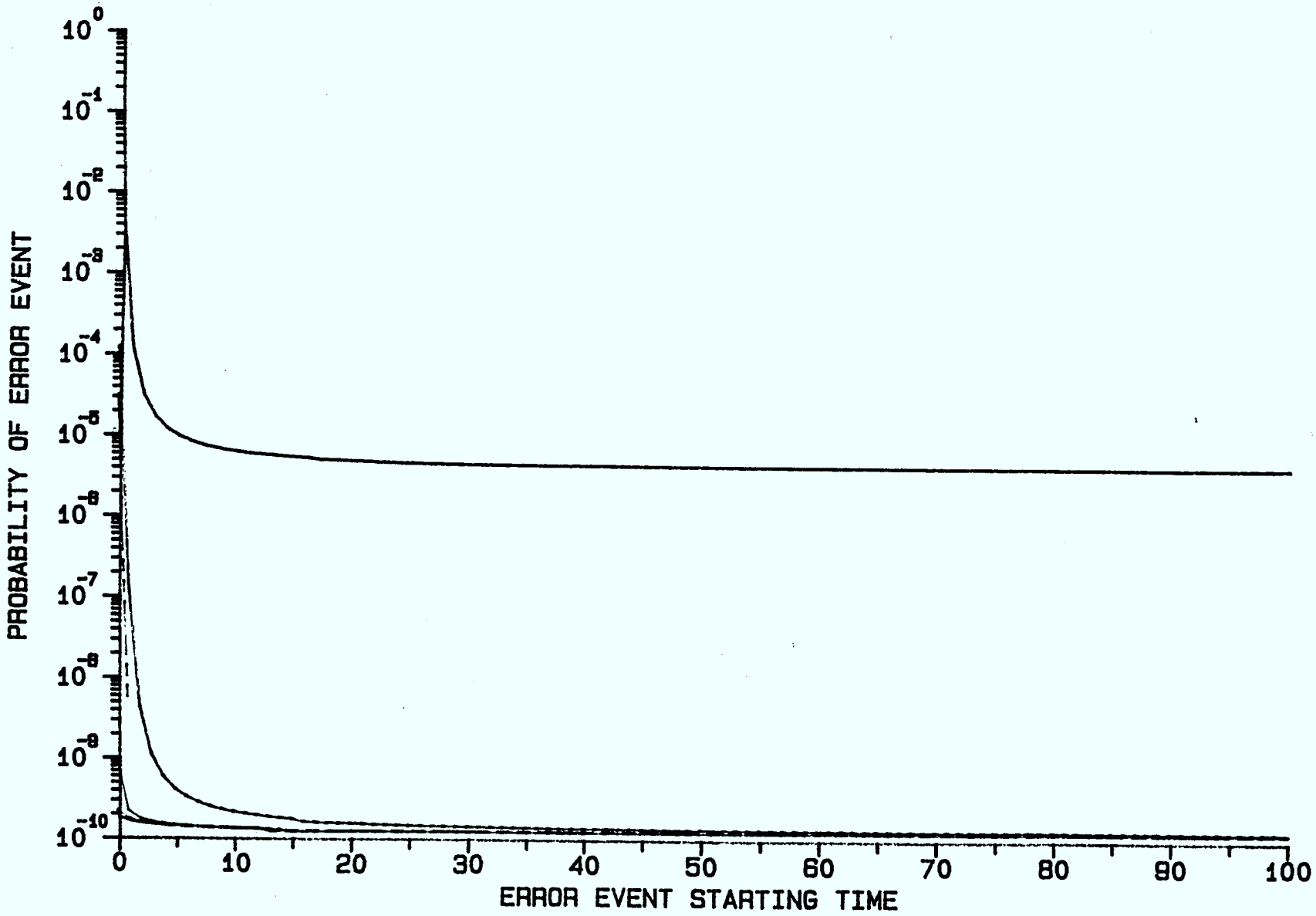

Fig.16 P_e for MSK

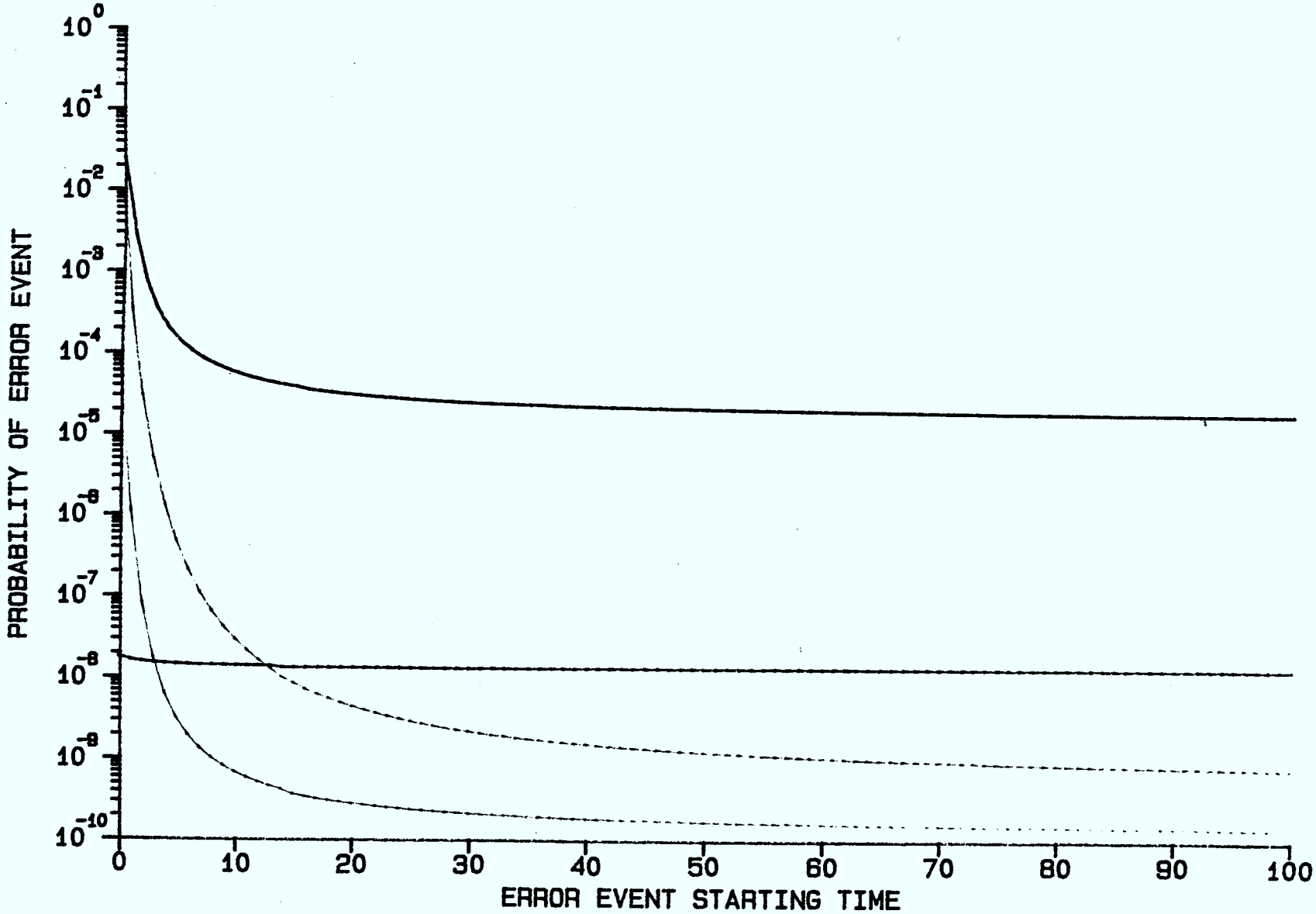

Fig. 17 P_e for DMSK

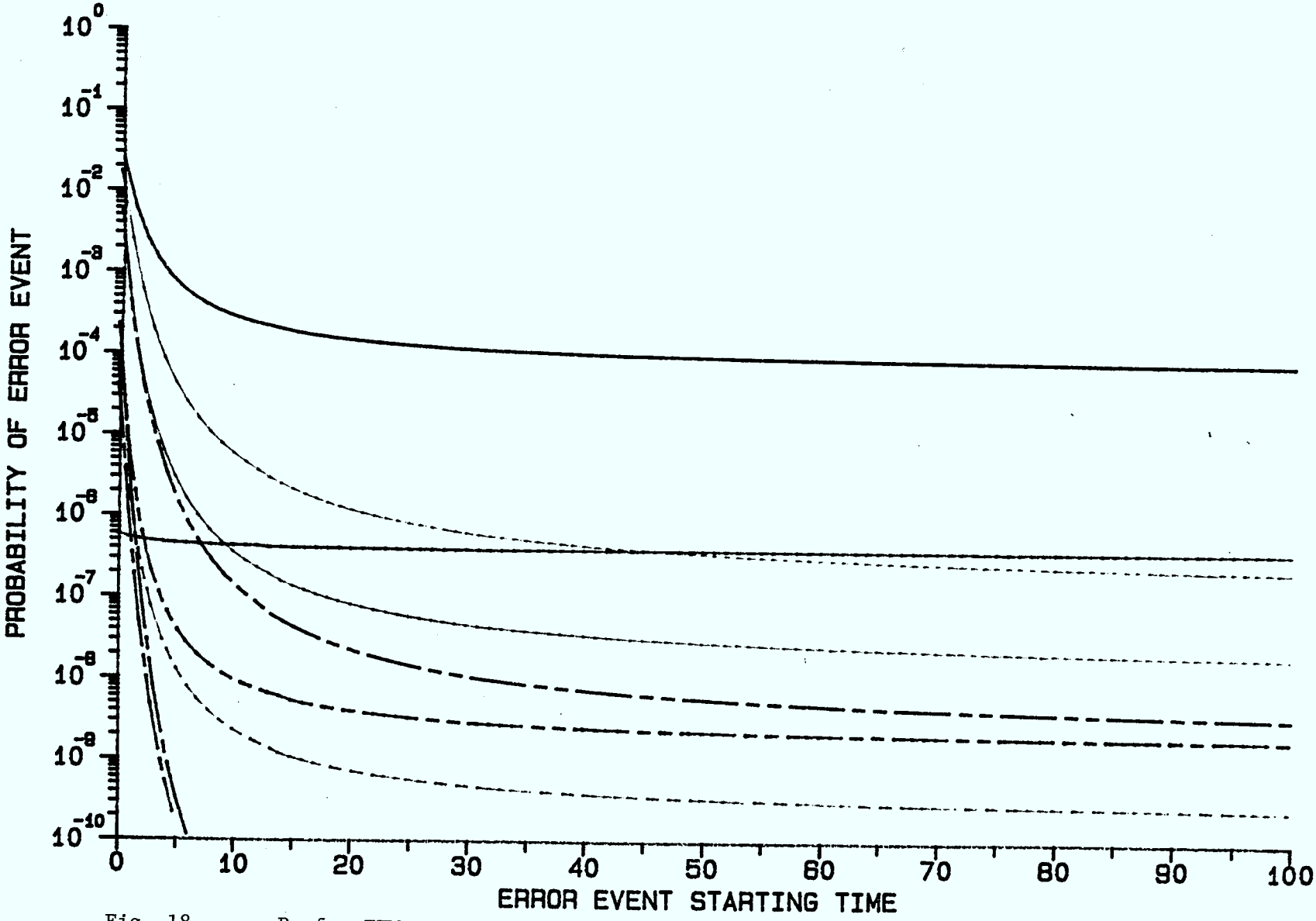

Fig. 18 P_e for TFM

4. OPTIMUM MLSE RECEIVER SPANNING FREQUENCY HOPS

4.1 INTRODUCTION

In Chapter Three the MLSE receiver that detects transmitted sequences of length less than or equal to the hop interval was presented. Such a receiver can be used to detect data on a hop-by-hop basis. We now extend the detection algorithm so that the receiver detects a transmitted sequence of arbitary length (greater than the hop length), based on the maximum likelihood accumulated over the entire transmission period. There will be periodic random phase jumps every NT seconds in the dehopped waveform. As one would expect, the receiver algorithm is more complex than the previous algorithm. However, a special case of the algorithm can be combined with the algorithm described in the previous chapter to give a simple practical algorithm for the situation where the hop interval is much longer than the length of the frequency pulse g(t).

4.2 RECEIVER THEORY

The received dehopped waveform is the same as that presented previously in Eq.(3.1)

$$r(t) = (2E/T)^{1/2} \sum_{i=-\infty}^{\infty} p(t-iNT) \cos [2\pi f_c t + \psi(t,\underline{\alpha}) + \theta_i] + n(t) \qquad (4.1)$$

where the symbols used are those defined and used previously. For a transmitted sequence of length n symbols and a hopping interval of length N, the number of phase jumps occurring would be the nearest

integer greater than n/N denoted by q.

Let the dehopped waveform be denoted by $s(t,\underline{\alpha},\underline{\theta})$, where $\underline{\theta}$ is a random vector, such that $s(t,\underline{\alpha},\underline{\theta}) = s(t,\underline{\alpha},\theta_i)$ for $iNT < t < (i+1)\,NT$. The detector must now find the sequence, of data symbols $\underline{\alpha}'$, which maximizes the likelihood function

$$\ell(\underline{\alpha},\underline{\alpha}') = E_{\underline{\theta}}\{e^{\frac{2a}{No}\int_o^{nT} r(t).s(t,\underline{\alpha}',\underline{\theta})\,dt}\} \tag{4.2}$$

Since the random initial phase θ_i's are statistically independent, the expectation can be taken over each hop interval independently as

$$\ell(\underline{\alpha},\underline{\alpha}') = \prod_{m=1}^{q} E_{\theta_{m-1}}\{e^{\frac{2a}{No}\int_{(m-1)NT}^{mNT} r(t)\, s(t,\underline{\alpha}',\theta_{m-1})dt}\} \tag{4.3}$$

where q is the least integer greater than n/N. The expectation over the random phase yields the zeroth-order modified Bessel function and the likelihood becomes

$$\ell(\underline{\alpha},\underline{\alpha}') = \prod_{m=1}^{q} I_o\{(2a/No)\,[\,\ell_{cm}^{2}(\underline{\alpha},\underline{\alpha}') + \ell_{sm}^{2}(\underline{\alpha},\underline{\alpha}')]^{1/2}\} \tag{4.4}$$

where

$$\ell_{cm}(\underline{\alpha},\underline{\alpha}') = \int_{(m-1)NT}^{mNT} r(t)\,\cos[2\pi f_c t + \psi(t,\underline{\alpha}')]dt \tag{4.5a}$$

$$\ell_{sm}(\underline{\alpha},\underline{\alpha}') = \int_{(m-1)NT}^{mNT} r(t)\,\sin[2\pi f_c t + \psi(t,\underline{\alpha}')]dt \tag{4.5b}$$

Comparing the likelihood function in Eq.(4.4) with that for $n \leq N$ given in Eq.(3.5), we see that the maximum likelihood decoding algorithm is now more complicated. The likelihood calculation involves multiplications, Bessel function weighting, squaring and square root

operations.

To reduce the number of multiplications involved, the log likelihood function may be used as given by

$$\Gamma(\underline{\alpha},\underline{\alpha}') = \sum_{m=1}^{q} \ln\{I_o[\frac{2a}{No}(\ell_{cm}^2(\underline{\alpha},\underline{\alpha}') + (\ell_{sm}^2(\underline{\alpha},\underline{\alpha}'))^{1/2}]\} \quad (4.6)$$

The computation in Eq.(4.6) can be carried out in a serial manner as follows. Initially during the first hop interval the equivalent likelihood given by Eq.(3.5) can be used to determine the most likely transmitted sequence in the first hop. Hence, the decoding algorithm can proceed in the same manner as for $n \leq N$ described in Section 3.3. At the end of the first hop, the decoder retains a list of survivors having the largest likelihood pairs $[\ell^*_{c,N}(j), \ell^*_{s,N}(j)]$ for each state at time NT. The decoder now has to compute

$$\Gamma_1(j) = \ln\{I_o[\frac{2a}{No}(\ell^*_{c,N}(j)^2 + \ell^*_{s,N}(j)^2)^{1/2}]\} \quad (4.7)$$

for each of the states $1 \leq j \leq \eta$. We shall refer to these as the partial log likelihoods accumulated over the first hop. To determine the survivors in the second hop for time $kT > NT$, the decoder must use the likelihood given by Eq. (4.6) rather than the equivalent likelihood $\ell'(\underline{\alpha},\underline{\alpha})$ as given by Eq. (3.5). Hence, to determine the survivor at time (N+1)T, the decoder computes the metric of the survivor at $S_{N+1} = j$ as

$$\ln \ell^*_{N+1}(j) = \max_i \{\Gamma_1(i) + \ln I_o[\frac{2a}{No}(\delta_c^2(i,j) + \delta_s^2(i,j))^{1/2}]\} \quad (4.8)$$

for $i=1,2,\ldots\eta$
$j=1,2,\ldots\eta$

where $\delta_c(i,j)$ and $\delta_s(i,j)$ are the inphase and quadrature matched filter outputs for the transition from node i to node j during a symbol interval. These are obtained in the same way as for the noncoherent receiver on a hop-by-hop detection basis presented previously.

For each of the nodes $S_{N+1} = j$, $1<j<\eta$, the inphase and quadrature registers for accumulating the inphase and quadrature correlations over the second hop, $\ell^*_{c,2,N+1}(j)$ and $\ell^*_{s,2,N+1}(j)$, are initialized as

$$\ell^*_{c,2,N+1}(j) = \delta_c(i,j) \tag{4.9a}$$

$$\ell^*_{s,2,N+1}(j) = \delta_s(i,j) \tag{4.9b}$$

Note that in the notation $\ell^*_{c,m,n}$ and $\ell^*_{s,m,n}$, a second subscript m, has been introduced to indicate that the m^{th} hop is under consideration and the subscript n, as before, indicates that the states at time nT are being evaluated. The partial log likelihood accumulated over the first hop for the survivor at node $S_{n+1} = j$ is also stored as

$$\Gamma^*_1(j) = \Gamma_1(i) \tag{4.10}$$

where i is the survivor state at time N and is the node index i that satisfies Eq. (4.8).

For $k > N+1$, laying in the second hop interval, the inphase and quadrature correlation calculations are the same as for the first hop except that comparison for determining the survivor at node $S_k = j$ is according to

$$\ell n\ \ell_k^*(j) = \max_i \{\Gamma_1^*(j) + \ell n\ I_o\{\frac{2a}{N_o}\ (\ell^*_{c,2,k-1}(i) + \delta_c(i,j)]^2 + [\ell^*_{s,2,k-1}(i) + \delta_s(i,j)]^2)^{1/2}\}\} \qquad (4.11)$$

The inphase and quadrature correlations are updated as

$$\ell^*_{c,2,k}(j) = \ell_{c,2,k-1}(i) + \delta_c(i,j) \qquad (4.12a)$$

$$\ell^*_{s,2,k}(j) = \ell_{s,2,k-1}(i) + \delta_c(i,j) \qquad (4.12b)$$

In general, for time k laying in the m^{th} hop other than the first hop, $(m-1)N < k < mN$, the metric of the node $S_k = j$ is defined as

$$\ell n\ \ell_k^*(j) = \max_i \{\Gamma^*_{m-1}(j) + \ell n\ I_o\{\frac{2a}{No}\ ([\ell^*_{c,m,k-1}(i) + \delta_c(i,j)]^2 + [\ell^*_{s,m,k-1}(i) + \delta_s(i,j)]^2)^{1/2}\ \}\ \} \qquad (4.13)$$

where $\Gamma^*_{m-1}(j)$ is the sum of the partial log likelihoods accumulated over the previous (m-1) hop intervals for the survivor ending at $S_k=j$, and is equal to

$$\Gamma^*_{m-1}(j) = \sum_{i=1}^{m-1} \Gamma_i^*(j) \qquad (4.14)$$

Note that the values a and N_o are required, which was not the case in the receiver considered in Chapter Three and the partial log likelihood sum $\Gamma^*_{m-1}(j)$ has to be stored in addition to the usual inphase and quadrature correlations $\ell^*_{c,m,k}(j)$and $\ell^*_{s,m,k}(j)$. Natural log and Bessel function weightings have to be performed. This dictates a more complex detection algorithm than previously obtained in hop-by-hop detection.

4.3 DECODER SIMPLIFICATION FOR L << N

If the length of the frequency pulse denoted by L is much less than the hop length N, then merges in the modulation trellis will usually occur much before the end of a hop. All the η different survivors at time kT, branch out from a common node, say S_t, where $(m-1)NT < t < kT$, hence $\Gamma^*_{m-1}(j)$ will be common to all the contending sequences.

$$\ell n \ell^*_k(j) = \max_i \{ \Gamma^*_{m-1}(j) + \ell n I_o \{ \frac{2a}{No} ([\ell_{c,m,k-1}(i) + \delta(i,j)]^2 + [\ell_{s,m,k-1}(i) + \delta_s(i,j)]^2)^{1/2} \} \}$$

$$= \max_i \{ \ell n I_o \{ \frac{2a}{No} ([\ell_{c,m,k-1}(i) + \delta(i,j)]^2 + [\ell_{s,m,k-1}(i) + \delta_s(k,j)]^2)^{1/2} \} \quad (4.15)$$

Hence once a merge has occurred within a hop the equivalent likelihood can be used for determining the maximum likelihood sequence via

$$\ell^{*'}_k(j) = \max_i \{ [\ell_{c,m,k-1}(i,j) + \delta_c(i,j)]^2 + [\ell_{s,m,k-1}(i,j) + \delta_s(i,j)]^2 \} \quad (4.16)$$

The decoding algorithm can then revert to the simple one as for the first hop. Note that the more complicated metric calculation in Eq. (4.13) is required only for a few symbol intervals after a frequency hop. Once a merge has occurred the comparison can then revert to the

simple one as in Eq.(4.16).

4.4 RECEIVER STRUCTURE

The only difference between the receiver obtained in this Chapter and the one discussed in previous chapters is the decoding algorithm. The receiver structure for generating $\delta_c(i,j)$ and $\delta_s(i,j)$ is the same as that presented in Chapter Three.

5.SUBOPTIMUM NONCOHERENT RECEIVER

5.1 INTRODUCTION

The noncoherent receiver described previously is quite complex, especially if the metric calculations are to be carried on across the hop intervals. A simplified sub-optimal receiver structure with reduced complexity may be obtained although error performance may be sacrificed. For the correlative encoded CPM signal described, there are correlator states (frequency states) as given by Eq. (3.8) and phase states as given by Eq. (3.9). If the phase states are ignored and only the correlator states are used to estimate the transmitted sequence, we have a simplified sub-optimum decision algorithm, which automatically takes care of the metric calculation across a frequency hop.

5.2 SUBOPTIMUM RECEIVER

The information carrying phase function $\psi(t)$ given in Eq. (3.7) can be alternatively expressed in term of the correlated data symbols

J_n as

$$\psi(t) = 2\pi h \sum_{n=o}^{\infty} J_n \, s(t-nT) \tag{5.1}$$

where J_n are the correlated data symbols given by

$$J_n = \frac{1}{C} \sum_{\ell=o}^{m} k_\ell \, \alpha_{n-\ell} \tag{5.2}$$

and

$$s(t) = \int_{-\infty}^{t} b(\tau) \, d\tau \tag{5.3}$$

where b(t) is the baseband pulse of length T. s(t) is normalized such that

$$s(T) = 1/2. \tag{5.4}$$

During the k^{th} symbol interval the information carrying phase function can be given by

$$\psi(t) = 2\pi \, h \, J_k \, s(t-kT) + \pi h \sum_{n=o}^{k-1} J_n \tag{5.5}$$

$$kT < t < (k+1)T$$

The underlying phase, which stays constant during the k^{th} symbol interval is then

$$\xi_k = \pi \, h \sum_{n=o}^{k-1} J_n + \theta_i \qquad i\,N < k < (i+1)\,N \tag{5.6}$$

Rather than having a random phase angle once per hop interval, we can assume for noncoherent bit detection that we have a noncoherent phase angle in each symbol interval. The suboptimum receiver must find the data sequence $\underline{\alpha}'$ that maximizes the following likelihood function.

$$\ell(\underline{a},\underline{a}') = E_{\xi}\{ \exp[(2a/N_o) \int_0^{nT} r(t)s(t,\underline{\alpha}',\xi)\, dt] \} \tag{5.7}$$

$$= \prod_{k=0}^{n-1} I_o\{(2a/N_o)\, z_k(\underline{\alpha}_k,\underline{\alpha}_k')\} \tag{5.8}$$

where

$$z_k(\underline{\alpha}_k,\underline{\alpha}_k') = [(\int_{kT}^{(k+1)T} r(t)\cos[2\pi f_c t + \beta_k(t,\underline{\alpha}')]dt)^2 + (\int_{kT}^{(k+1)T} r(t)\sin[2\pi f_c t + \beta_k(t,\underline{\alpha}')]dt)^2]^{1/2} \tag{5.9}$$

and $\beta_k(t,\underline{\alpha}')$ is the shape of the phase path during the k^{th} symbol interval due to the k^{th} correlated symbol J_k' given by

$$\beta_k(t,\underline{\alpha}') = 2\pi h\, J_k'\, s(t-kT) \tag{5.10}$$

and

$$J_k' = \frac{1}{C} \sum_{\ell=o}^{m} k_\ell\, \alpha'_{k-\ell} \tag{5.11}$$

For M-ary transmission and a PRS polynomial of degree m, there would be at most M^m states rather than pM^m states for the MLSE receiver presented in the previous Chapter. The memory and computational requirement is then reduced.

Instead of having the likelihood function as a product of Rician variables $z_k(\underline{\alpha},\underline{\alpha}')$, the log likelihood function can be used as given by

$$\Gamma(\underline{\alpha},\underline{\alpha}') = \sum_{k=o}^{n-1} \ell n[I_o\{(2a/No)\, z_k\, (\underline{\alpha},\underline{\alpha}')\}] \tag{5.12}$$

The Viterbi algorithm can be used for calculating the metric recursively through

$$\Gamma_k^*(j) = \max_i \{\Gamma_{k-1}^*(i) + z_k(i,j)\} \tag{5.13}$$

where $\Gamma^*_{k-1}(i)$ is the metric of the survivor node $S_{k-1}=i$ and $z_k(i,j)$ is the Rician variable for transition from node i to node j corresponding to that given by Eq. (5.9).

5.3 SUBOPTIMUM RECEIVER STRUCTURE

Since the phase path $\beta_k(t,\underline{\alpha}')$ during a symbol interval depends on the correlated symbol J_k only, the number of possible distinct phase paths is the number of possible distinct correlated symbols. The receiver structure must be able to provide the partial log likelihood $\ell n I_o\{(2a/No).z_k(\underline{\alpha},\underline{\alpha}')\}$ for every possible phase path during a symbol interval. Following approach used in section 3.4, we have

$$\int_{kKT}^{(k+1)T} r(t)\cos[2\pi f_c t + \beta_{ki}(t)]\,dt$$

$$= \int_{kT}^{(k+1)T} r_c(t)\cos\beta_{ki}(t)\,dt - \int_{kT}^{(k+1)T} r_s(t)\sin\beta_{ki}(t)dt \tag{5.14}$$

and

$$\int_{kT}^{(k+1)T} r(t)\sin[2\pi f_c t + \beta_{ki}(t)]dt$$

$$= \int_{kT}^{(k+1)T} r_c(t)\sin\beta_{ki}(t)dt + \int_{kT}^{(k+1)T} r_s(t)\cos\beta_{ki}(t)\,dt \tag{5.15}$$

where

$$r_c(t) = r(t)\cos 2\pi f_c t$$

$$r_s(t) = r(t)\sin 2\pi f_c t \tag{5.16}$$

A baseband matched filter bank is then required to provide the

correlations with the cosine and sine of all possible phase paths $\beta_{ki}(t)$ over each symbol interval. For the correlation with the cosine of the i^{th} possible phase path, the matched filter impulse response is

$$h_{ci}(t) = \cos\,[\beta_{ki}(T-t)]$$

$$= \begin{cases} \cos\,[2\pi h\, J_i\, s(T-t)] & 0 < t < T \\ 0 & \text{elsewhere} \end{cases} \qquad (5.17)$$

and the matched filter impulse response for the correlation with the sine of the i^{th} possible phase path is

$$h_{si}(t) = \sin\,[\beta_{ki}(T-t)]$$

$$= \begin{cases} \sin\,[2\pi\, J_i\, s(T-t)] & 0 < t < T \\ 0 & \text{elsewhere} \end{cases} \qquad (5.18)$$

Comparing Eqs.(5.14) and (5.15) with Eqs.(3.19) and (3.20), we see that this suboptimum receiver requires the same number of matched filters as the MLSE receiver. The scaling multipliers for the MLSE receiver are not required but squaring operations and summers are required as well as the weightings $\ell n I_o[(2a/No)\sqrt{(\ )}]$. Note that although the receiver may look as complex as the MLSE receiver, the function weighting is now being done in hardware which can be much faster. In the case where the software can handle the required mathematical operations, the structure of the receiver is much simpler indeed. The receiver block diagram is as shown in Fig.19.

6. CONCLUSIONS

Spectral analysis of frequency-hopped, correlative encoded continuous phase modulations has been presented. Results on the power

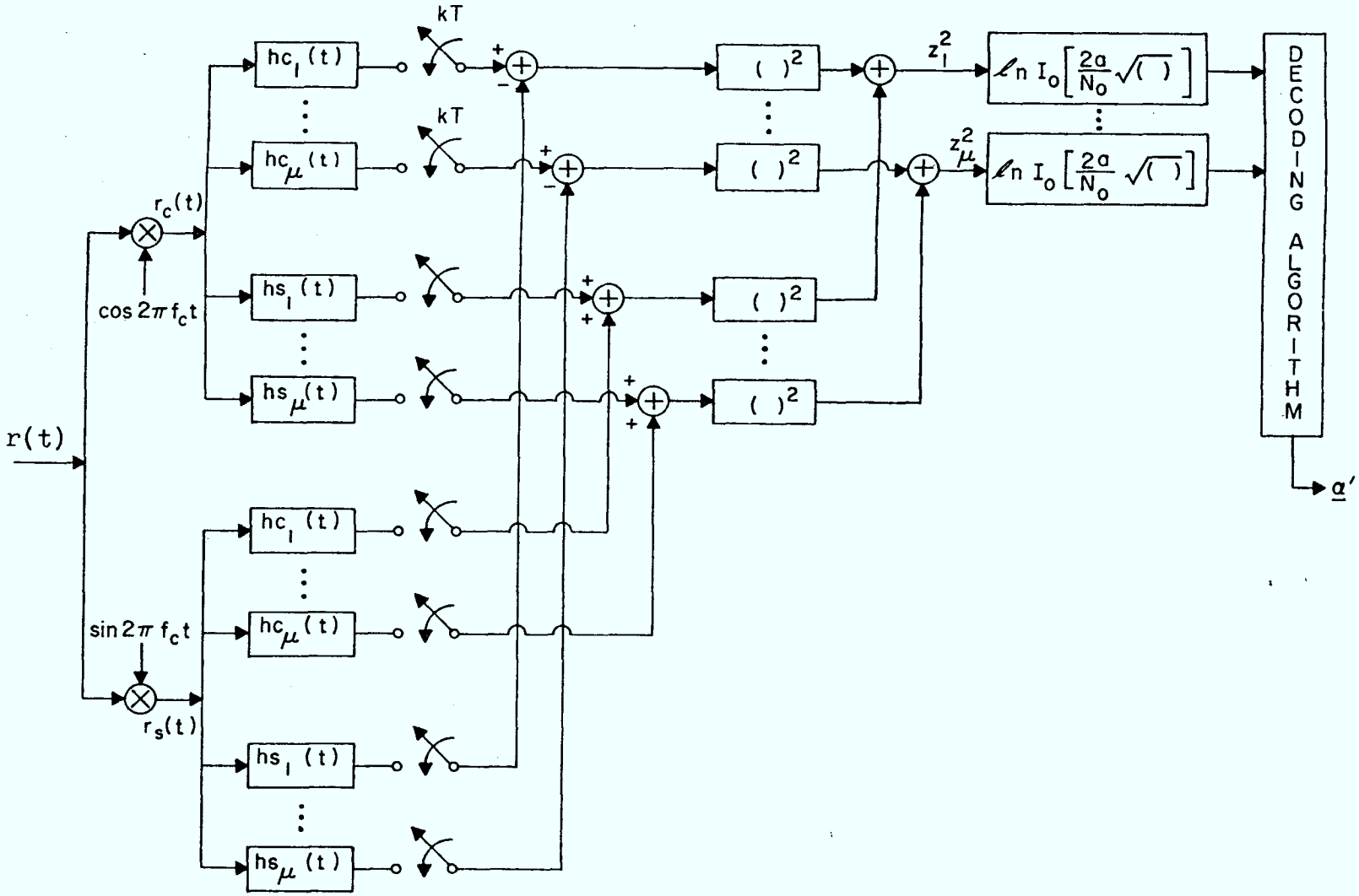

Fig. 19 SUBOPTIMUM ML RECEIVER BLOCK DIAGRAM

density spectra of frequency-hopped signals with various partial response encodings and pulse shaping, and different hop lengths have been presented. In general, the spectrum becomes more compact with lower sidelobes and approaches that of the CPM signal without hopping, as the length of the hop interval increases.

It is found that the use of higher order PRS polynomials and pulse shaping, which are known to reduce the bandwidth significantly for usual continuous phase modulation, do not result in more compact spectra if the hop length is short. The use of higher order PRS polynomials and pulse shaping is effective in bandwidth and sidelobe reduction for long hop intervals.

Three noncoherent receivers have been presented. The maximum likelihood receiver presented in Chapter Three is optimum over a single hop interval. Consequently it can be used for sequence estimation on a hop-by-hop basis. It has the simplest receiver structure and decoding algorithm. Error performance of this receiver has been analysed. It has higher error probability at the beginning and near the end of a hop. If some channel throughput can be sacrificed, known symbols can be transmitted at the end of a hop to force a merge in the modulation trellis at the end of each hop.

In Chapter Four, the MLSE receiver that detects a general frequency-hopped signal has been presented. It has the same structure as the one that detects on a hop-by-hop basis but it has a more complicated decoding algorithm. However, simplification of the decoding algorithm is possible when the length of the hop interval is much greater than the length of the frequency pulse. The receiver operates generally in the same manner as the single hop receiver, but it has a subprocedure

for metric calculation across each frequency hop and relies on the assumption that a merge in the trellis will occur well before the end of a hop.

In Chapter Five, an additional simplified suboptimum receiver has been presented. For this receiver a different structure is required and the decoding algorithm is simpler. Memory requirements and computation are reduced.

Error performance analysis of the single-hop receiver has been presented.

7. REFERENCES

1. C.E. Cook and H.S. Marsh, "An Introduction to Spread Sprectrum", IEEE Communications Magazine, Vol. 21, No. 2, pp. 8-16, March 1983.

2. T. Aulin, N. Rybeck and C-E. Sundberg, "Bandwidth Efficient Digital FM with Coherent Phase Tree Demodulation", Technical Report TR-102, May 1978, Telecommunication Theory, University of Lund, Lund.

3. G.S. Deshpande and P.H. Wittke, "Correlative Encoded Digital FM", IEEE Trans. on Comm., Vol. COM-29, pp. 156-162, Feb. 1981.

4. P. Kabal and S. Pasupathy, "Partial-Response Signaling", IEEE Trans. on Comm. Vol. COM-23, pp. 921-934, Sept. 1975.

5. T. Aulin and C-E. Sundberg, "Numerical Calculation of Spectra for Digital FM Signals", National Telecommunications Conference, NTC´81, New Orleans, Louisianna, November 29 - December 3, 1981, Conference Record, pp. D8.3.1-D8.3.7.

6. T. Aulin and C-E. Sundberg, "An easy way to calculate power spectra for digital FM", IEE Proceedings, Vol. 130, Part f, No. 6, pp. 519-526, Oct. 1983.

7. W.P. Osborne and M.B. Luntz, "Coherent and Non-coherent Detection of CPFSK", IEEE Trans. on Comm., Vol. COM-22, pp. 1023-1036, August 1974.

8. T.A. Schonhoff, "Symbol Error Probabilities for M-ary CPFSK: Coherent and Non-coherent Detection", IEEE Trans. on Comm., Vol. COM-24, pp. 644-652, July 1976.

9. T. Aulin and C-E. Sundberg, "On Partially Coherent Detection of Digital Continuous Phase Modulation Signals", Technical Report TR-127, May 1979, Telecommunication Theory, University of Lund, Lund.

10. A. Svensson and C-E. Sundberg, "Error Probability Bounds for Noncoherently Detected CPM", Technical Report TR-183, August 1984, Telecommunication Theory, University of Lund.

11. A. Svensson and C-E. Sundberg, "On Error Probability for Several Types of Noncoherent Detection of CPM", IEEE GLOBECOM'84, Conference Record, pp. 22.5.1-22.5.7.

12. G.D. Forney, "Maximum-Likelihood Sequence Estimation of Digital Sequences in the Presence of Intersymbol Interference", IEEE Trans. on Information Theory, Vol. IT-18, pp. 363-378, May 1972.

13. G.D. Forney, "The Viterbi Algorithm", Proc. of the IEEE, Vol. 61, No. 3, pp. 268-278, March 1973.

14. S.J. Simmons and P.H. Wittke, "Low Complexity Decoder for Constant Envelope Digital Modulations", IEEE Trans. on Comm., Vol. COM-31, No. 12, pp. 1273-1280, Dec. 1983.

15. P.J. McLane, "The Viterbi Receiver for Correlative Encoded MSK Signals", IEEE Trans. on Comm., Vol. COM-31, No. 2, pp. 290-295, Feb. 1983.

16. H. Kobayashi, "Correlative Level Coding and Maximum-Likelihood Decoding", IEEE Trans. on Information Theory, Vol. IT-17, No. 5, pp. 586-594, Sept. 1971.

17. P.H. Wittke, P.J. McLane, S.J. Simmons and Y.M. Lam, "A Bandwidth Efficient Frequency-Hopped Spread Sprectrum Modulation Study", Dept. of Elect. Eng., Queen's University, Resarch Report No. 85-03, March 1985.

18. W.F. McGee, "Another Recursive Method of Computing the Q Function", IEEE Trans. on Information Theory, Vo. IT, pp. 500-501, July 1970.

II. TRELLIS CODING FOR HOPPED SPREAD SPECTRUM SYSTEMS

1. INTRODUCTION

The implementation of satellite communication systems usually proves challenging due to the modest power available for down-link transmission. Thus it is highly desirable to minimize the energy per bit required to provide communication at the specified level of error performance. This consideration certainly holds for EHF military satellite communications, where the trend is to communication at higher and higher frequencies over wide bandwidths - at frequencies where it is a technical challenge to produce signal sources of even modest level. Thus any technique such as coding that could reduce the required energy per bit, would seem worthy of consideration. In addition a reduced vulnerability to jamming could accrue.

The common applications of coding and coded modulations have been to the additive Gaussian noise channel where a coherent modulation and demodulation has been possible. For example the Trellis codes of Ungerboeck [1], have been applied to 8-phase PSK and 16 point Quadrature Amplitude Modulation, to achieve coding gains of the order of 3-4 dB with no penalty in transmission rate. These codes are now being used in commercial data transmission equipment. However, for communications in the EHF band, coherent techniques do not appear possible and it is a challenge to find effective coding and decoding techniques that use noncoherent detection. In this report we provide the principles and first results of work that has been started on a coded Noncoherent Frequency Shift Keying (NC-FSK) modulation that

promises coding gains of the order of 3-4 dB as has been achieved with trellis codes and coherent systems. In addition, because the basic modulation is a noncoherent M-ary FSK, the use of existing spectrum analyzer receivers appears possible.

2. RESULTS

The basic uncoded modulation system from which the coded system is derived, is a noncoherent M-ary FSK in which one of M orthogonal tones is transmitted in each baud interval. Cases are being considered where M = 2,4,8. The coding technique being applied, is analogous in a sense to that used by Ungerboeck for coherent transmission, where he obtained coding gain by use of a convolutional code, but avoided a lowering of transmission rate by increasing the number of points in the signal constellation to compensate for the redundancy in the code.

Here we introduce a convolutional encoding but suffer no rate reduction because we allow simultaneous use of more than one tone in the orthogonal signal set. If it is desired to control the maximum amplitude variation permissible, it is possible to place a constraint on the number of tones used. For example, in an eight tone system, the constraint could be to encode by the particular choice of four out of the eight possible tones.

Although our fundamental goal is to evaluate the performance for noncoherent reception, the error performance for coherent reception is relatively easy to analyse and so this analysis is being carried out as well. The error performance of the coded systems is being compared with uncoded M-ary FSK for which the theoretical error performance is

known. Also simulation results due to Keightley [2] are available and are being used for comparison.

The optimum receivers for the encoded multitone signals have been obtained in a straightforward manner. For noncoherent reception, the receiver consists of a conventional inphase and quadrature spectrum analyzer receiver. Samples of the inphase and quadrature components at the various frequencies are taken for processing by the decoder which is a Viterbi decoder.

Trellis coding can be considered as a binary convolutional encoding with a mapping of the encoded bits into an expanded set of channel signals. Rate 1/2, 2/3 and 3/4 codes with various constraint lengths are being studied with both hard and soft decisions at the output of the spectrum analyzer and input to the decoder. We have been able to show that the Euclidean distance in the FSK signal set is proportional to the Hamming distance in the modulating binary signal set. Thus for the modulation scheme being considered, optimal codes are obtained by maximizing d_{free}. An upper bound on the error performance for the coded system has been obtained from the code generating function and the probability of error for the uncoded system. This requires computer evaluation. As well, a computer simulation is being carried out to corroborate the theoretical work. Coding gains of the order of 3 dB. are being obtained, much the same as in the coherent Ungerboeck encoding.

3. REFERENCES

1. G. Ungerboeck, "Channel Coding with Multilevel/Phase Signals", IEEE Trans. on Information Theory, Vol. IT-28, No.1, pp.55-66, January 1982.

2. R.J. Keightley, "A Simulation of Frequency-Dehopped Binary and 4-ary NC-FSK Signals", Communications Research Centre, Ottawa, Canada, Tech. Note, No.722, April 1984.